SW trending quartz veins/veinlets which are probably conjugate. A 1 m thick quartz vein was identified at the southeastern part of the area and trends N30° E dipping around 65 degrees NW.

2-1-4 Sampling

Sampling was done in two areas; the reconnaissance survey area and the detailed survey area. The latter area was selected on the results of the sampling and geological survey of the former area. Sampling was done in grid system.

Baseline was established in N-S direction and sampling lines were set perpendicular to the baseline at spacing of 100 m in the reconnaissance area and at spacing of 50 m in the detailed area. The number of lines was 13 in the reconnaissance area and 8 in the detailed area. Sampling was undergone along sampling lines at intervals of 50 m and 10-20 m, respectively. Baselines, sampling lines and points were surveyed by compass and measuring tape. The extensions of the area were 1.6 km by 1.6 km and 400 m by 500 m. The number of samples was 345 and 328 (Total 673 samples). At each sampling point, 1 kg of soil sample was taken from B horizon. After air-drying, samples were sieved. About 100 g of minus 80 mesh fraction was taken for each sample and they were split in two parts; one part for the Philippines and the other part for the Japanese survey team and were later analyzed.

2-1-5 Pathfinder Elements and Method of Chemical Analysis

Au and Cu were expected to occur in this area. Thus the following 11 elements were selected as pathfinder elements; Au, Ag, Cu, As, Fe, Hg, Mo, Pb, S, Sb, Zn.

Neutron activation analysis was applied for analysis of Au. Induction furnace method was applied for analysis of S. ICP-AES method was applied for the other nine elements.

The lower detection limits for each element were as follows; Au: 1 ppb, Ag: 0.2 ppm, As, Pb, Sb, Zn: 2 ppm, Fe: 1 ppm and S: 0.01 %.

2-1-6 Analysis of Geochemical Data

Analytical values were converted into natural logarithms. Half of the value of the lower limit has been used for convergence of statistical processing.

(1) Statistical Processing: The basic statistical values of the elements were shown in Table 6. In the basic statistical values of each element, natural value is expressed in maximum and minimum values. The mean is expressed in natural values and logarithmic values, while standard deviation is expressed in logarithmic values.

Table 6 Basic Statistic Values of Elements on Geochemical Analysis

Element	Unit	Maximum	Minimum	Average	Ave.(-Log)	Std. Dev.
Au	ppb	2600	<1	38.59	11.2924	0.5622
Ag	ppm	0.4	<0.2	0.11	0.1047	0.0894
As	ppm	28	<2	5.08	3.7007	0.3625
Cu	ppm	316	89	178.06	175.1664	0.0856
Fe	%	10.7	3.68	6.39	6.3257	0.0687
Hg	ppm	3	<1	0.55	0.5345	0.0976
Mo	ppm	2	<1	0.61	0.5772	0.1326
Pb	ppm	22	2	8.60	8.0345	0.1647
S	%	0.09	<0.01	0.04	0.0349	0.1655
Sb	ppm	10	<2	1.75	1.4691	0.2347
Zn	ppm	186	20	76.20	72.2102	0.1561

The maximum and mean values are; Au 2,600 ppb and 38.6 ppb, Cu 316 ppm and 178 ppm, Pb 22 ppm and 8.6 ppm, Zn 186 ppm and 76.2 ppm. Compared with Clarke number, Au is dozens times, Cu is around 3 times, Pb is one tenth, and Zn is about unity. Therefore, only Au is selected as the most important mineralization in the area.

The values of Ag, Hg and Mo are very low and most values are below the detection limit of analysis. Thus, these elements were excluded from the data analysis.

The correlation coefficients were shown in Table 7. There is no element correlating with Au. The correlation is not recognized in each element excepting for Fe and S which have weak positive correlation.

Table 7 Correlation Coefficients among each Element on Geochemical Analysis

	Au	As	Cu	Fe	Pb	S	Sb	Zn
Au	1.000							
As	-0.011	1.000						
Cu	-0.001	0.040	1.000					
Fe	-0.040	-0.017	0.104	1.000				
Pb	0.095	-0.036	0.286	0.003	1.000			
S	0.014	0.086	0.122	0.346	0.227	1.000		
Sb	-0.037	-0.075	-0.026	0.107	-0.007	-0.038	1.000	
Zn	0.038	-0.057	0.215	-0.146	-0.078	-0.353	0.030	1.000

(2) Classification of Geochemical Anomaly Values: In this survey, mean and standard deviation together with frequency and cumulative frequency curve have been used to establish the threshold value. The frequency distributions and the cumulative frequency distributions in each element were shown in Fig. 7. The classification is based on 1/2 σ. The classification of geochemical anomalies were shown in Table 8. For all elements, more than two steps of classifications are set to distinguish the high anomalies.

Table 8 Classifications of Geochemical Anomalies

Au	M(11.3ppb), M+ σ (41.2ppb), M+2 σ (150.4ppb), M+2.5 σ (287.2ppb)
As	M+0.5 σ (5.6ppm), M+ σ (8.5ppm), M+1.5 σ (12.9ppm)
Cu	M(175.2ppm), M+ σ (213.3ppm), M+2 σ (259.8ppm)
Fe	M+0.5 σ (6.85%), M+1.5 σ (8.02%), M+2 σ (8.68%)
Pb	M+0.5 σ (9.7ppm), M+1.5 σ (14.2ppm)
S	M(0.035%), M+ σ (0.051%)
Sb	M(1.5ppm), M+2 σ (4.3ppm)
Zn	M(72.2ppm), M+ σ (103.5ppm)

(3) Distribution of Geochemical Anomalies: Distributions of geochemical anomalies were shown in Fig. 8. As to gold anomaly, the magnified figure of the detailed survey area was made.

[Au] The high anomalies are distributed near the diorite body or along the NNE-SSW oriented fault passing by the ridge of peak 379 m. The high Au concentration area is also recognized in the silicified zone which is distributed along the eastern side of Kampayas creek and in the upper stream of Kampayas creek corresponding to the southern part of the survey area.

[As] Though the high concentration areas are distributed from the ridge of peak 379 m to the northern part, there is no significant anomaly as a whole.

[Cu] The values of Cu show high concentration in all samples. Slightly higher concentration area is distributed near the diorite body at the ridge around peak 379 m.

[Fe] This element shows the high concentration at the propylitic alteration parts with pyritization such as the silicified zone at the eastern part of Kampayas creek. The slightly high concentration area also exists around the ridge of peak 379 m.

[Pb] The values of Pb show low concentration in all samples. The slightly high concentration area, however, is distributed from the ridge of peak 379 m to the southern part.

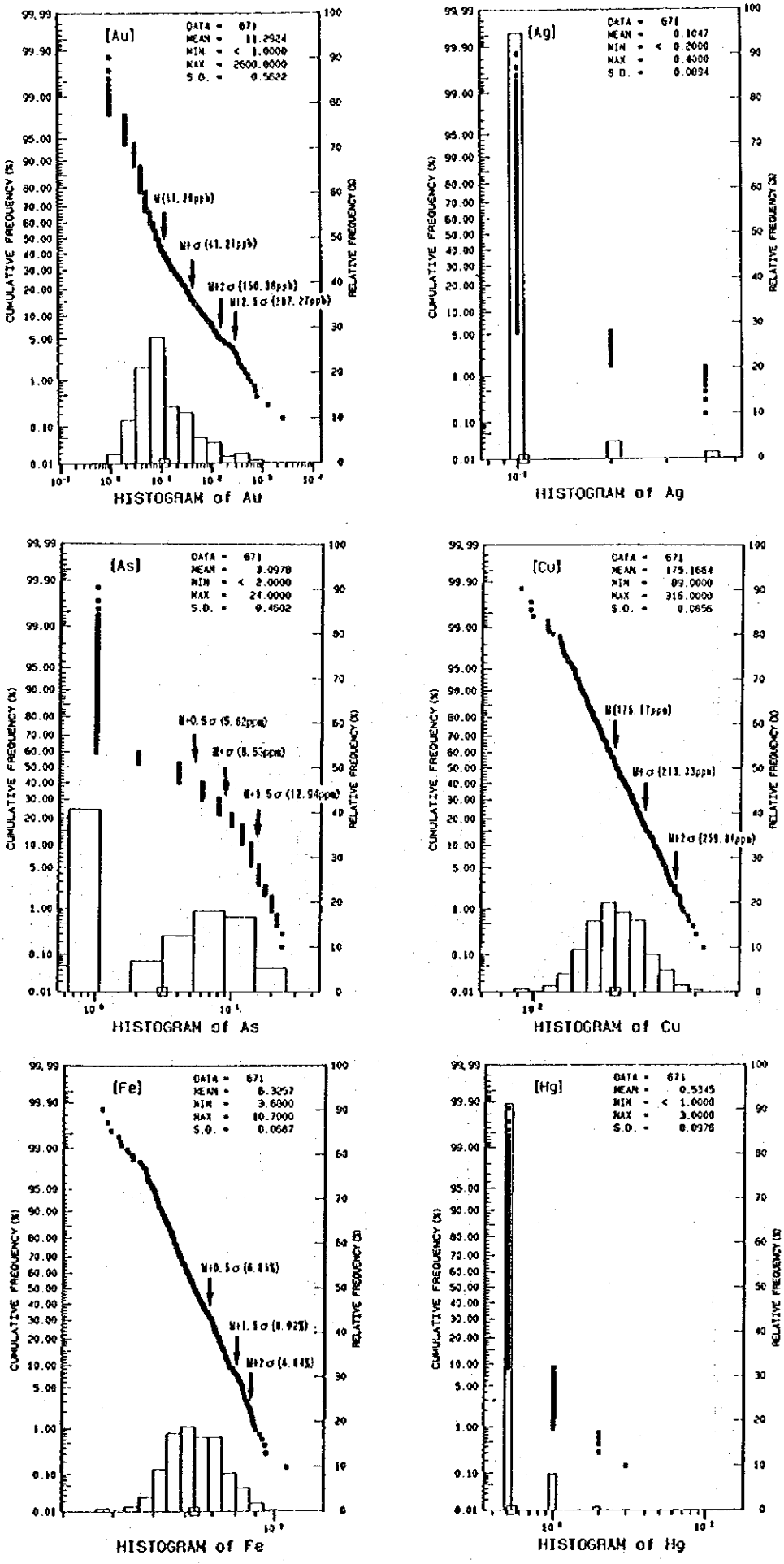

Fig. 7 Frequency Distribution and Cumulative Frequency Distribution (1)

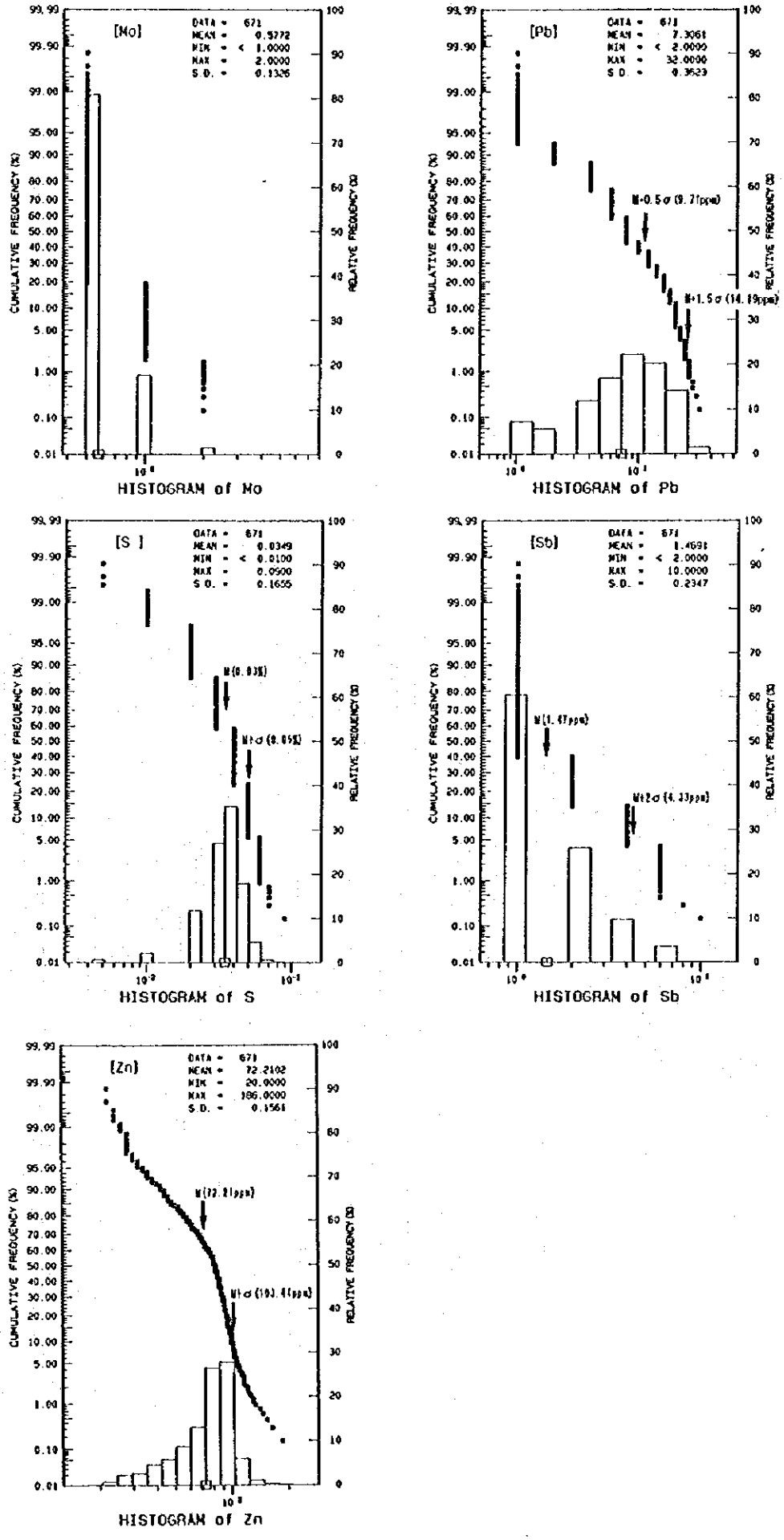

Fig. 7 Frequency Distribution and Cumulative Frequency Distribution (2)

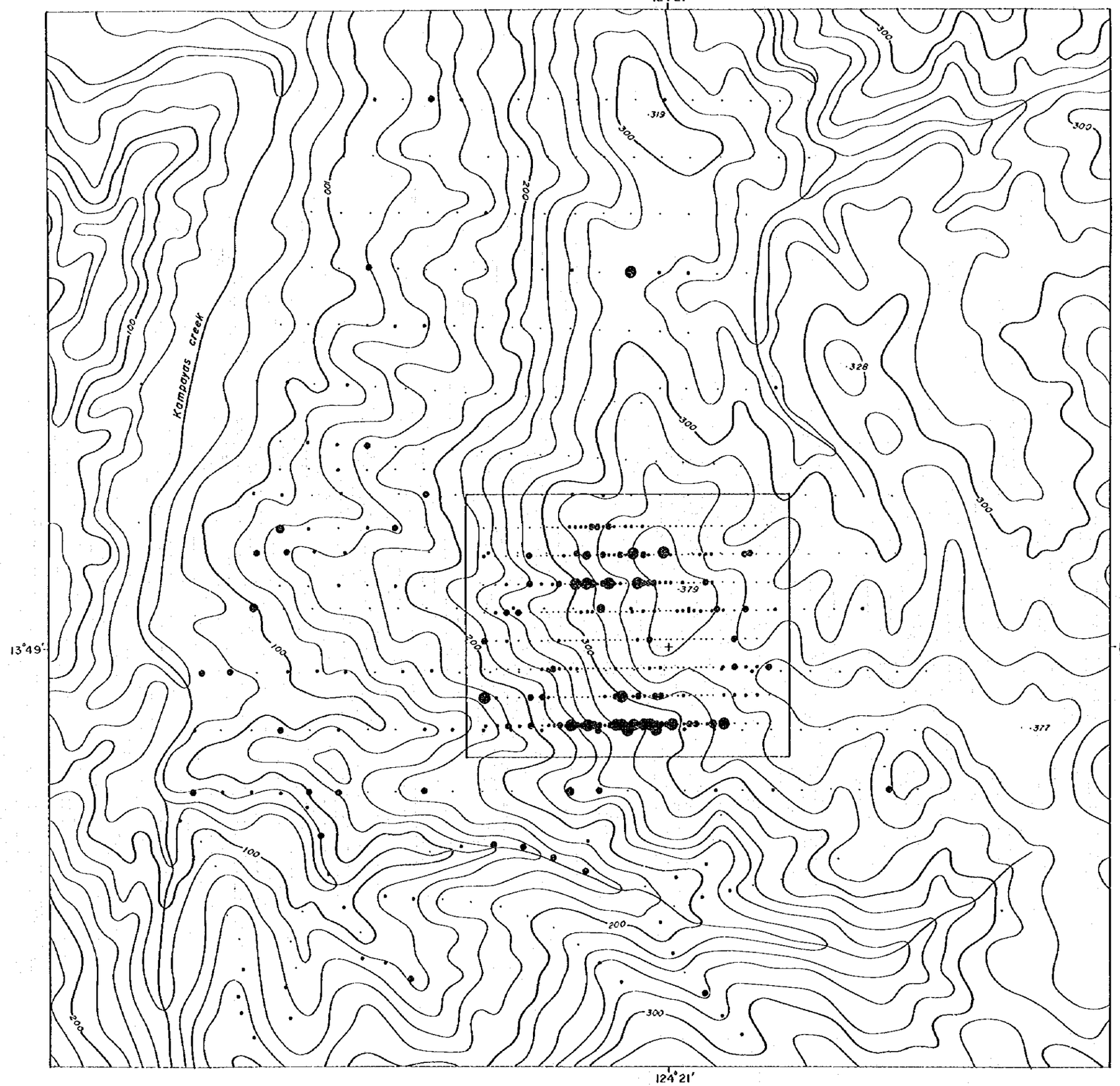

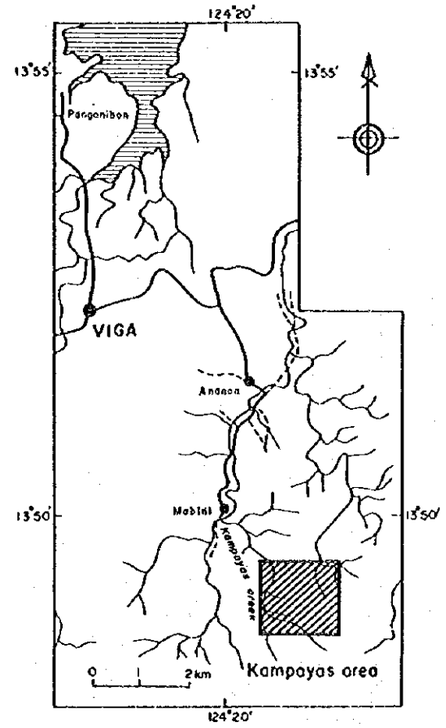

Au (ppb)

. : < 11.282

• : < 41.205

● : < 150.355

● : < 287.211

● : > 287.211

0 100 200 300 400 500m

Fig. 8 Distribution of Geochemical Anomalies (1)

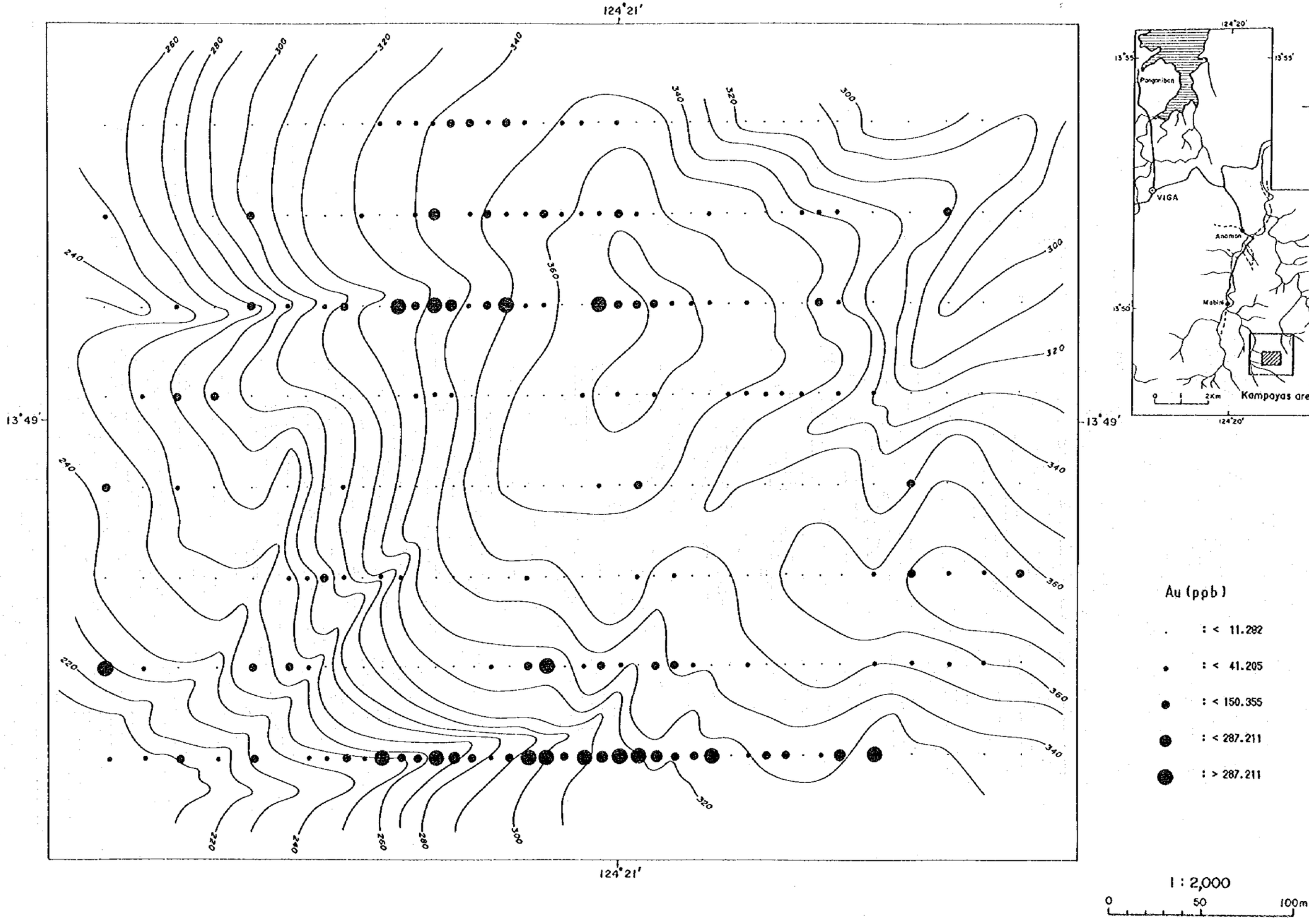

Fig. 8 Distribution of Geochemical Anomalies (2)

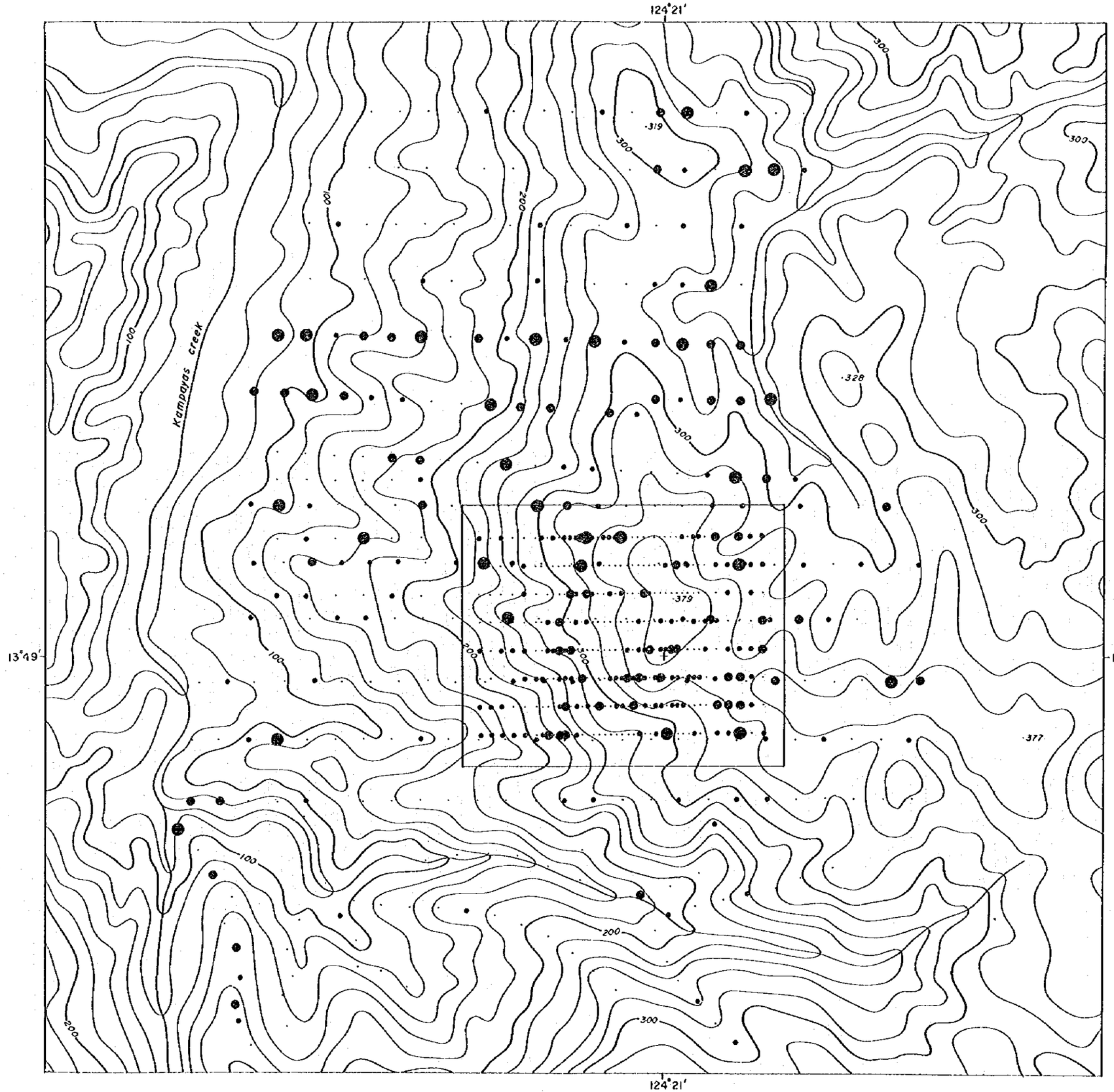

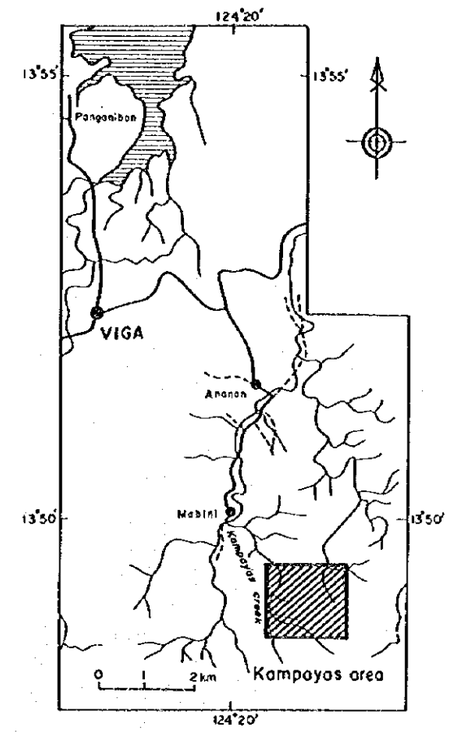

As (ppm)

. : < 5.617

• : < 8.527

● : < 12.943

● : > 12.943

0 100 200 300 400 500m

Fig. 8 Distribution of Geochemical Anomalies (3)

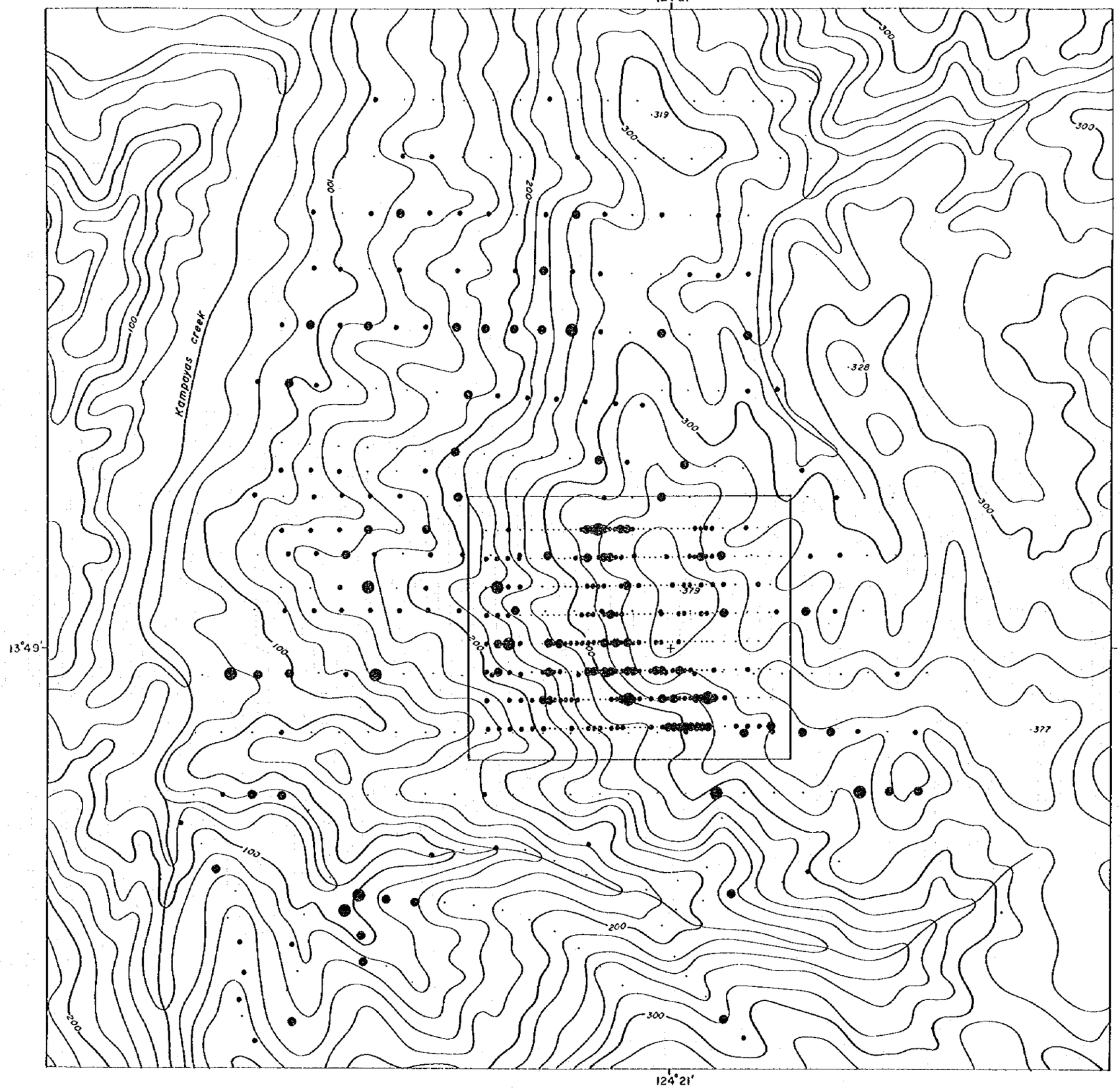

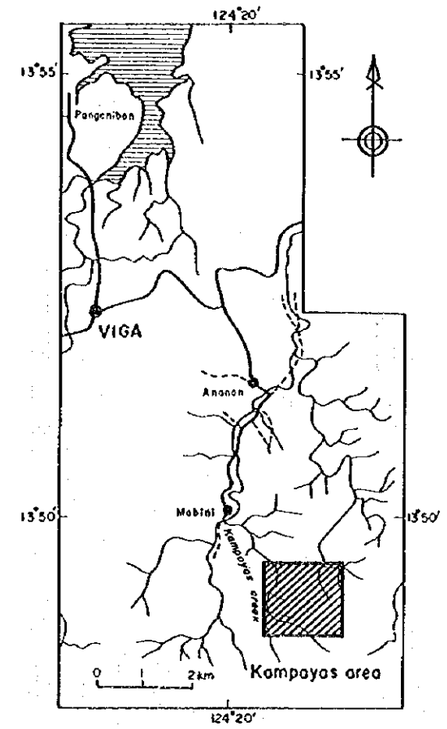

Cu (ppm)

. : < 175.166

• : < 213.345

● : < 259.846

● : > 259.846

0 100 200 300 400 500m

Fig. 8 Distribution of Geochemical Anomalies (4)

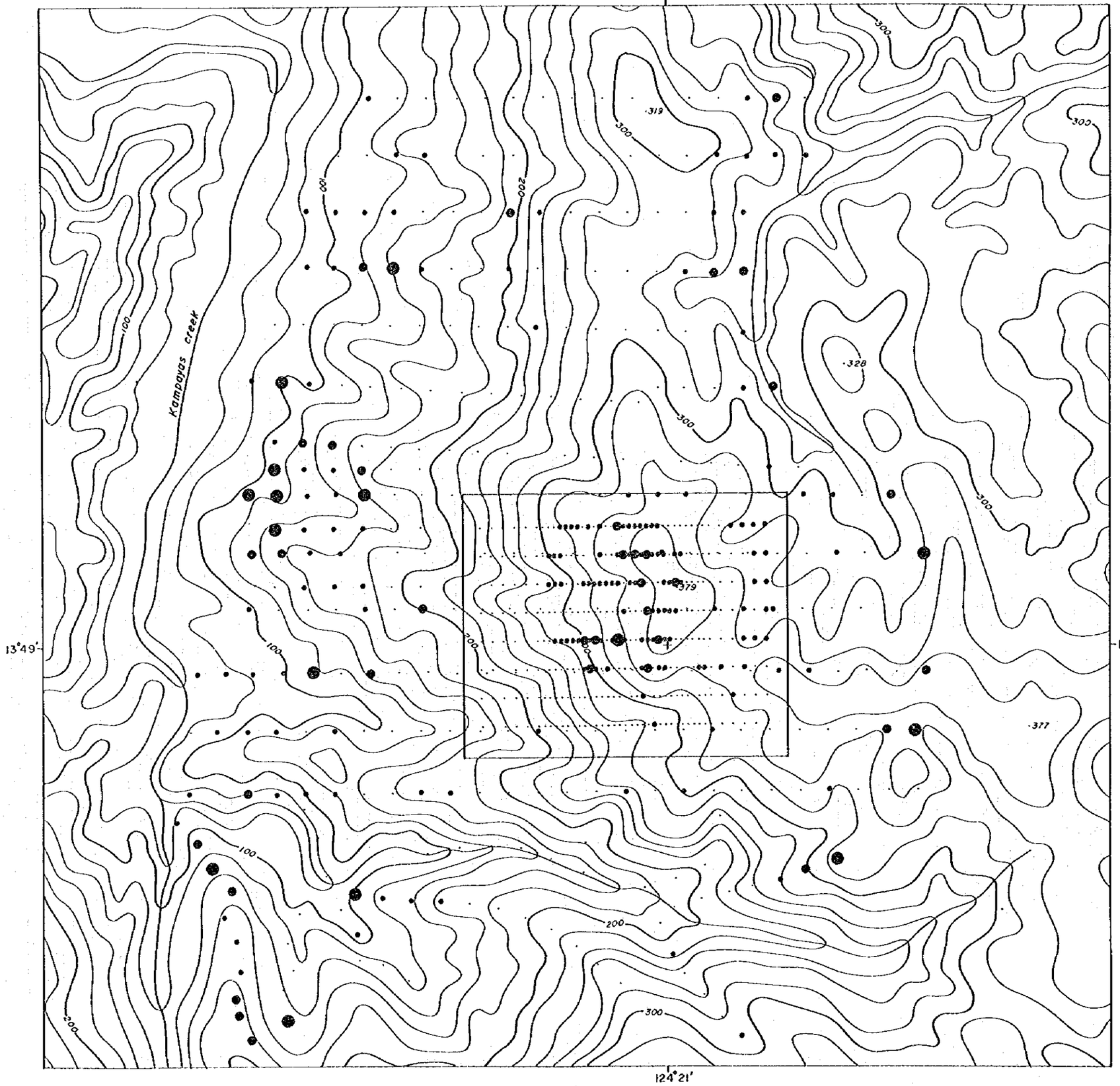

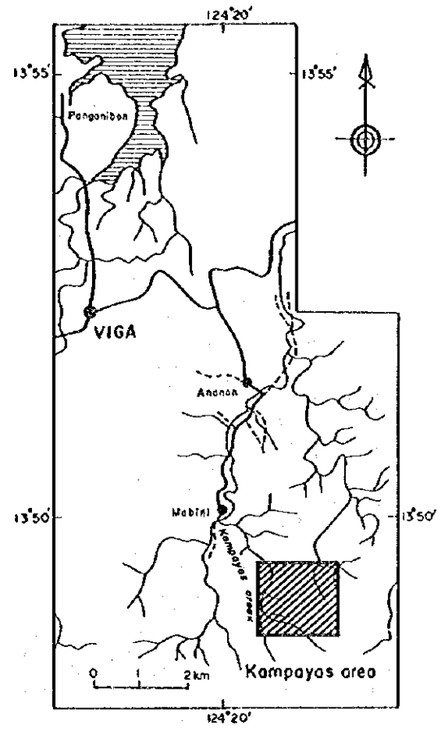

Fe (%)

. : < 6.848

• : < 8.019

● : < 8.678

● : > 8.678

0 100 200 300 400 500m

Fig. 8 Distribution of Geochemical Anomalies (5)

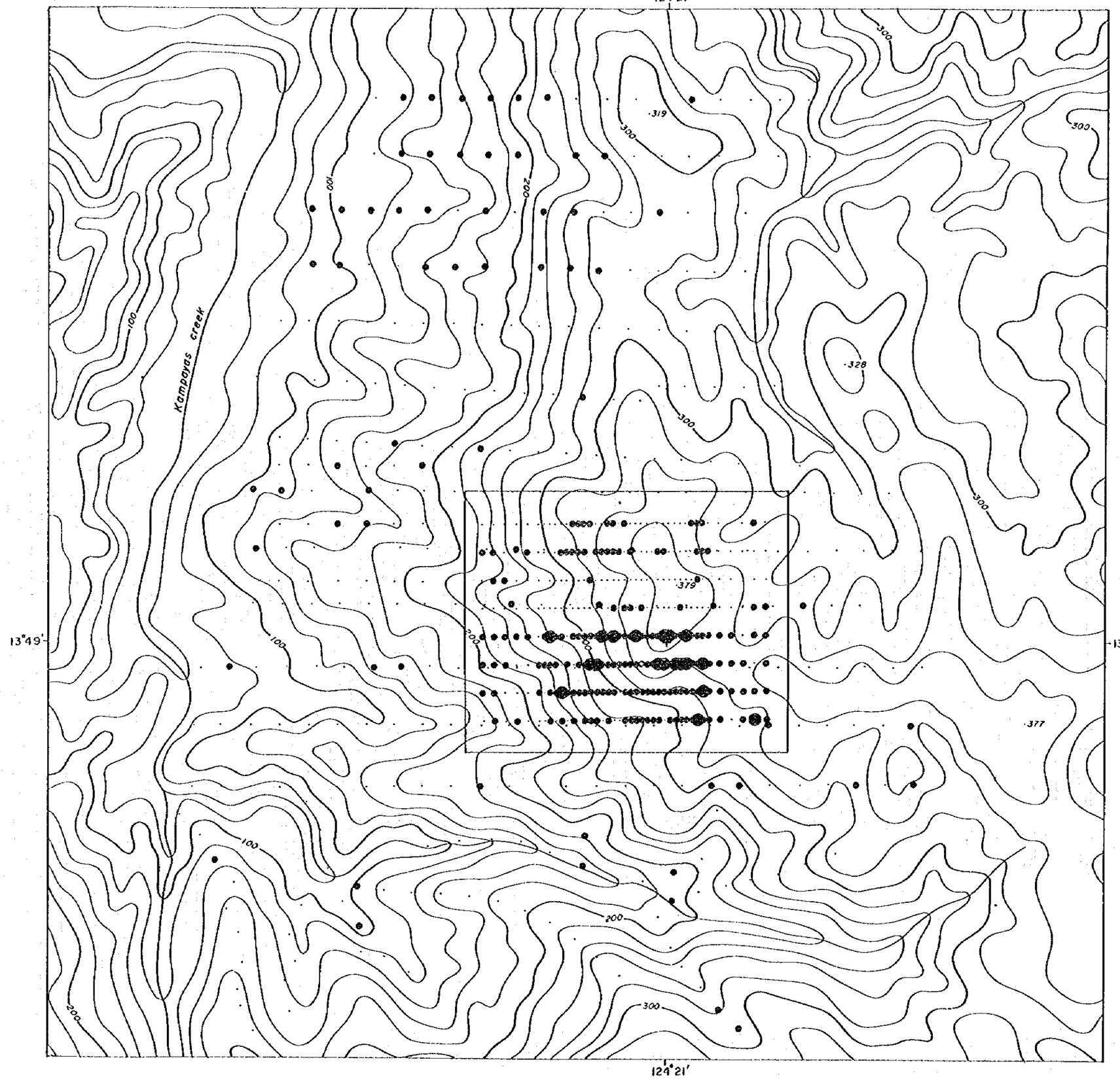

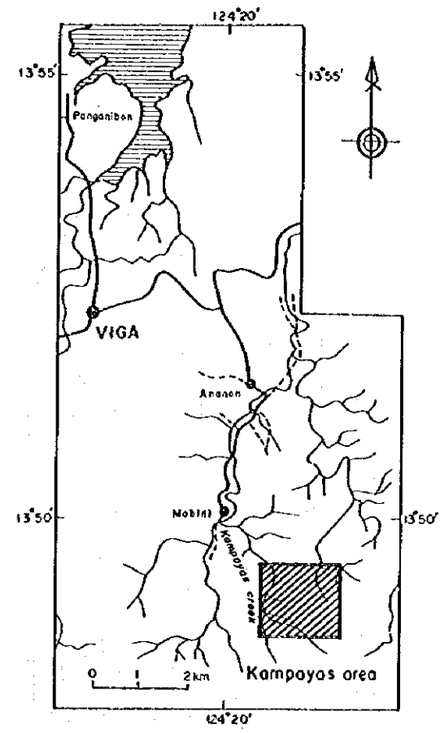

Pb (ppm)

. : < 8.035

• : < 14.182

: > 14.182

0 100 200 300 400 500m

Fig. 8 Distribution of Geochemical Anomalies (6)

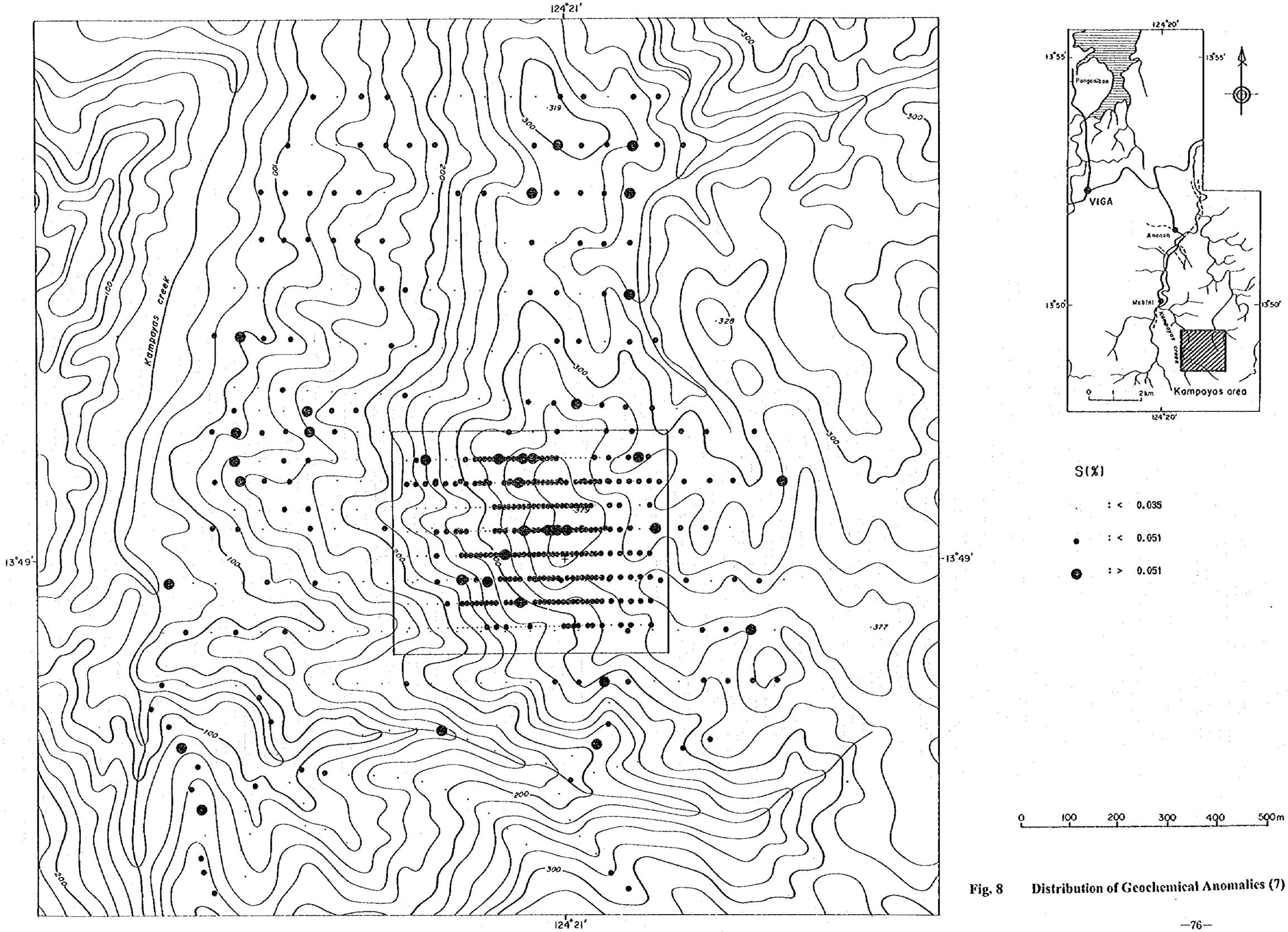

Fig. 8 Distribution of Geochemical Anomalies (7)

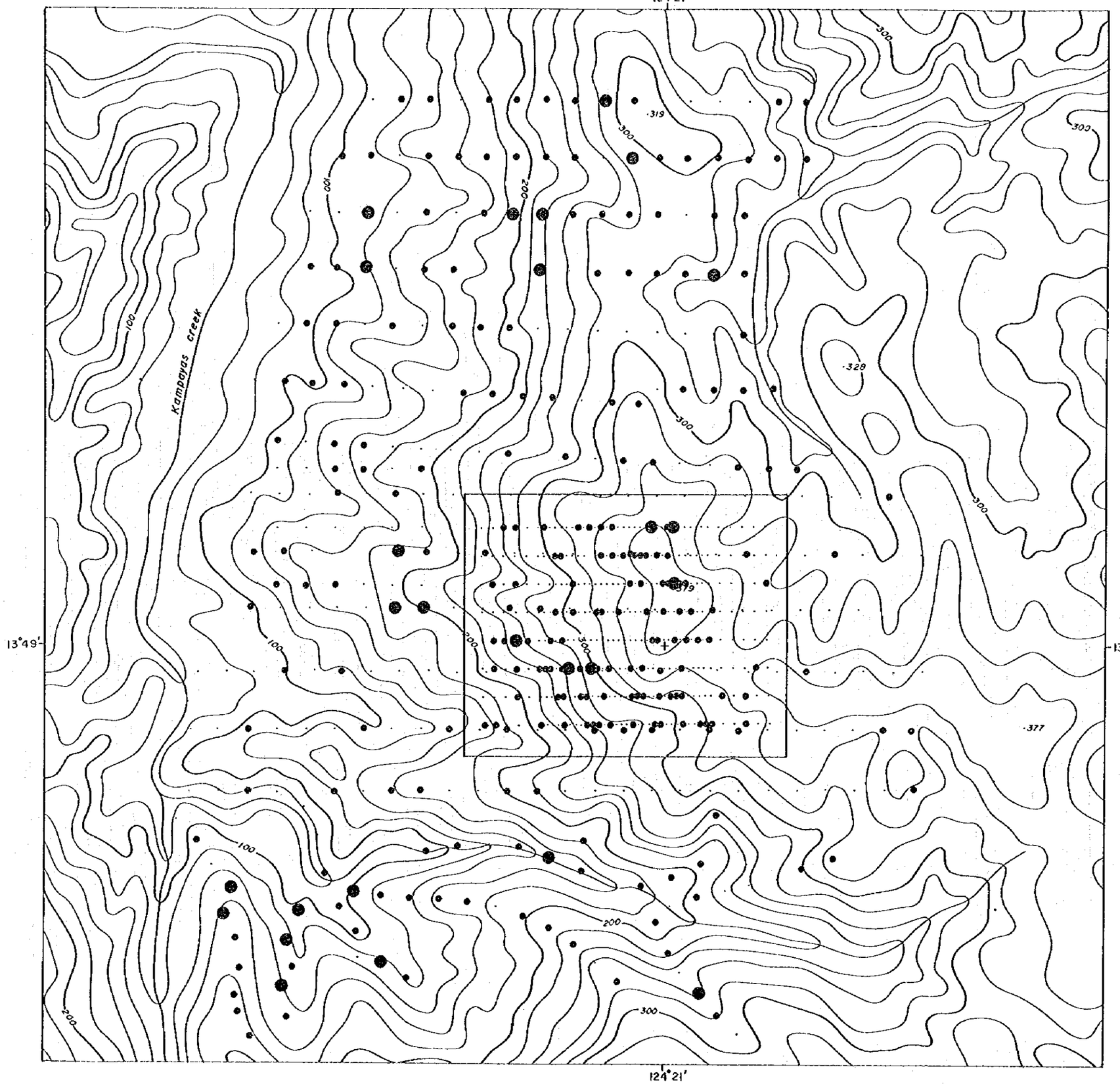

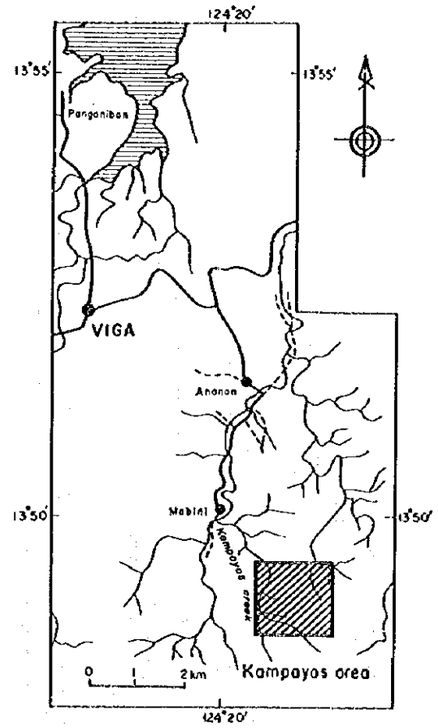

Sb (ppm)

. : < 1.489

: < 4.329

: > 4.329

0 100 200 300 400 500m

Fig. 8 Distribution of Geochemical Anomalies (8)

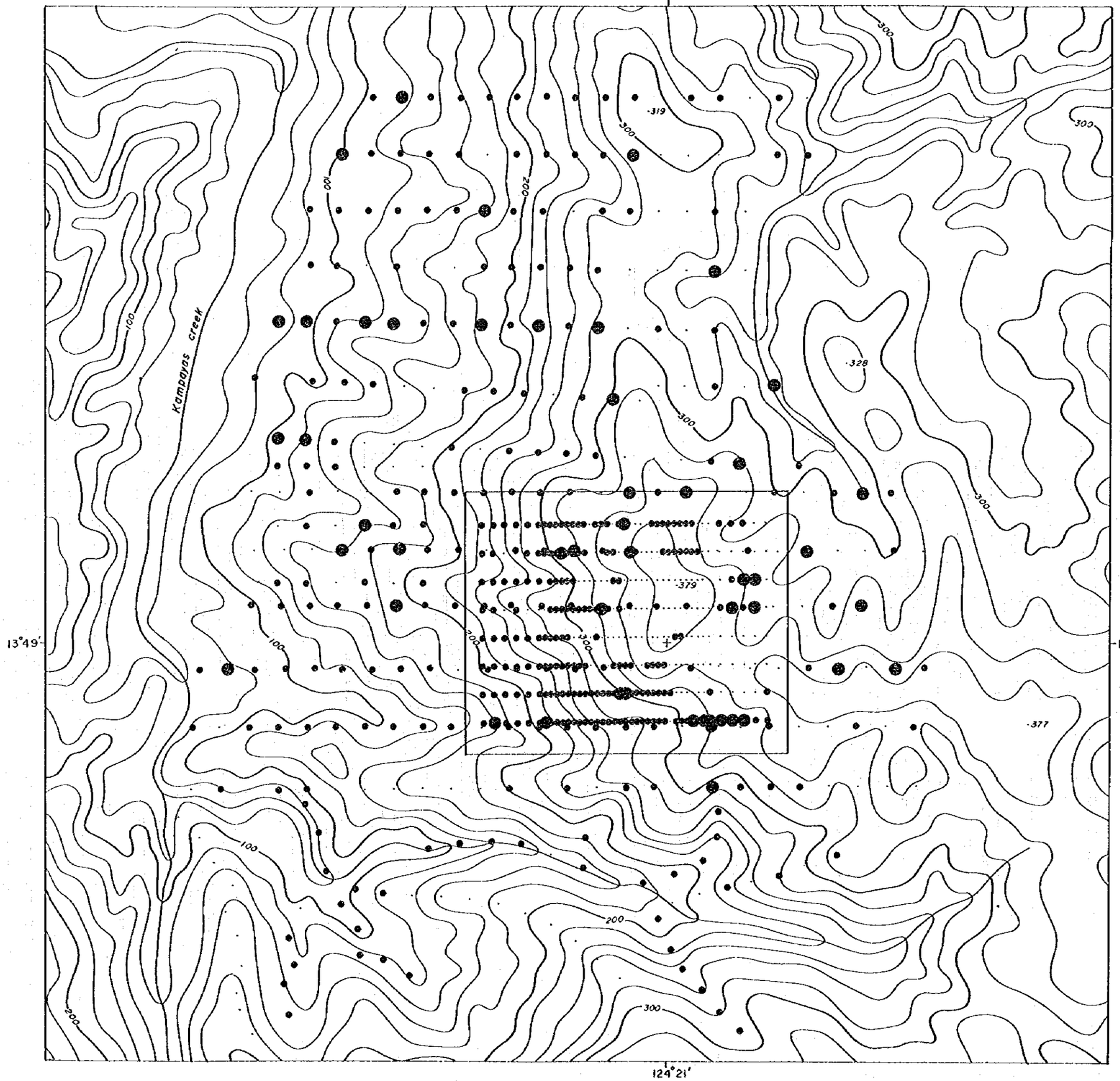

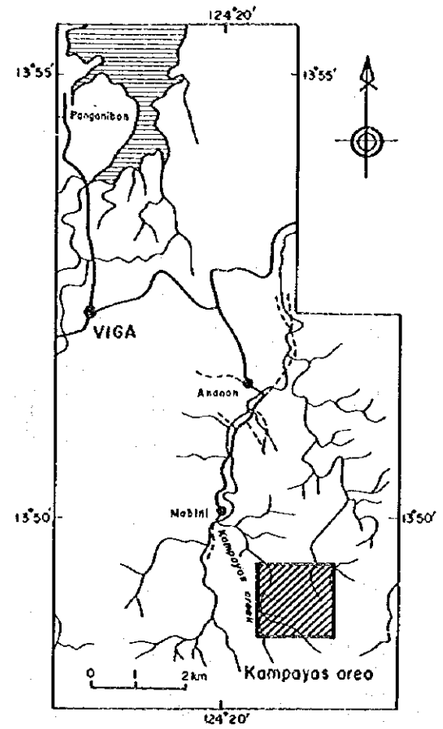

Zn (ppm)

. : < 72.210

: < 103.455

: > 103.455

0 100 200 300 400 500m

Fig. 8 Distribution of Geochemical Anomalies (9)

[S] This element shows the high concentration at the propylitic alteration parts with pyritization such as the silicified zone at the eastern part of Kampayas creek. The slightly high concentration area also exists around the ridge of peak 379 m.

[Sb] The values of Sb show low concentration in all samples. Thus, there is no trend as to Sb.

[Zn] Most of the values of Zn show low concentration within the diorite body at the ridge around peak 379 m.

(4) Multivariant Analysis (Principal Component Analysis): Principal component analysis was accomplished in order to see if there are groups of elements with correlative behavior and what control their grouping. Correlation coefficients (Table 7) are used for the calculation of the principal component analysis. The results of the analysis and score distributions were shown in Table 9 and Fig. 9.

The eigenvalue is 1.66 and contribution is 20.79 % for first principal component as shown in Table 9. Up to fourth principal component, each eigenvalue is almost over 1.0 and cumulative contribution is 64.6 %. Accordingly, from the first to fourth principal components are enough to explain the important behaviors of each element. Following each principal component has such characters mentioned below;

Table 9 Results of Principal Component Analysis (PCA)

Eigenvalue				Factor Loading				
P.C.	E.V.	Con.	Cum.Con.		Z-01	Z-02	Z-03	Z-04
Z-01	1.663	20.789	20.789	S	0.833	-0.088	0.061	0.005
Z-02	1.329	16.608	37.397	Fe	0.596	-0.143	-0.431	-0.143
Z-03	1.137	14.213	51.610	Cu	0.278	0.773	-0.109	-0.320
Z-04	1.038	12.972	64.582	Zn	-0.550	0.566	-0.208	-0.212
Z-05	0.923	11.537	76.119	Pb	0.467	0.557	0.100	0.260
Z-06	0.866	10.823	86.942	Sb	-0.007	-0.070	-0.736	0.106
Z-07	0.539	6.740	93.682	Au	0.014	0.249	0.305	0.667
Z-08	0.506	6.319	100.000	As	0.131	-0.074	0.498	-0.588

First principal component: This component has largely positive factor loadings of Fe and S. These elements may relate to propylitic alteration with large amount of pyrite. High scores are distributed near the ridge of peak 379 m and its northeastern part, and near the silicified zone at the eastern part of Kampayas creek.

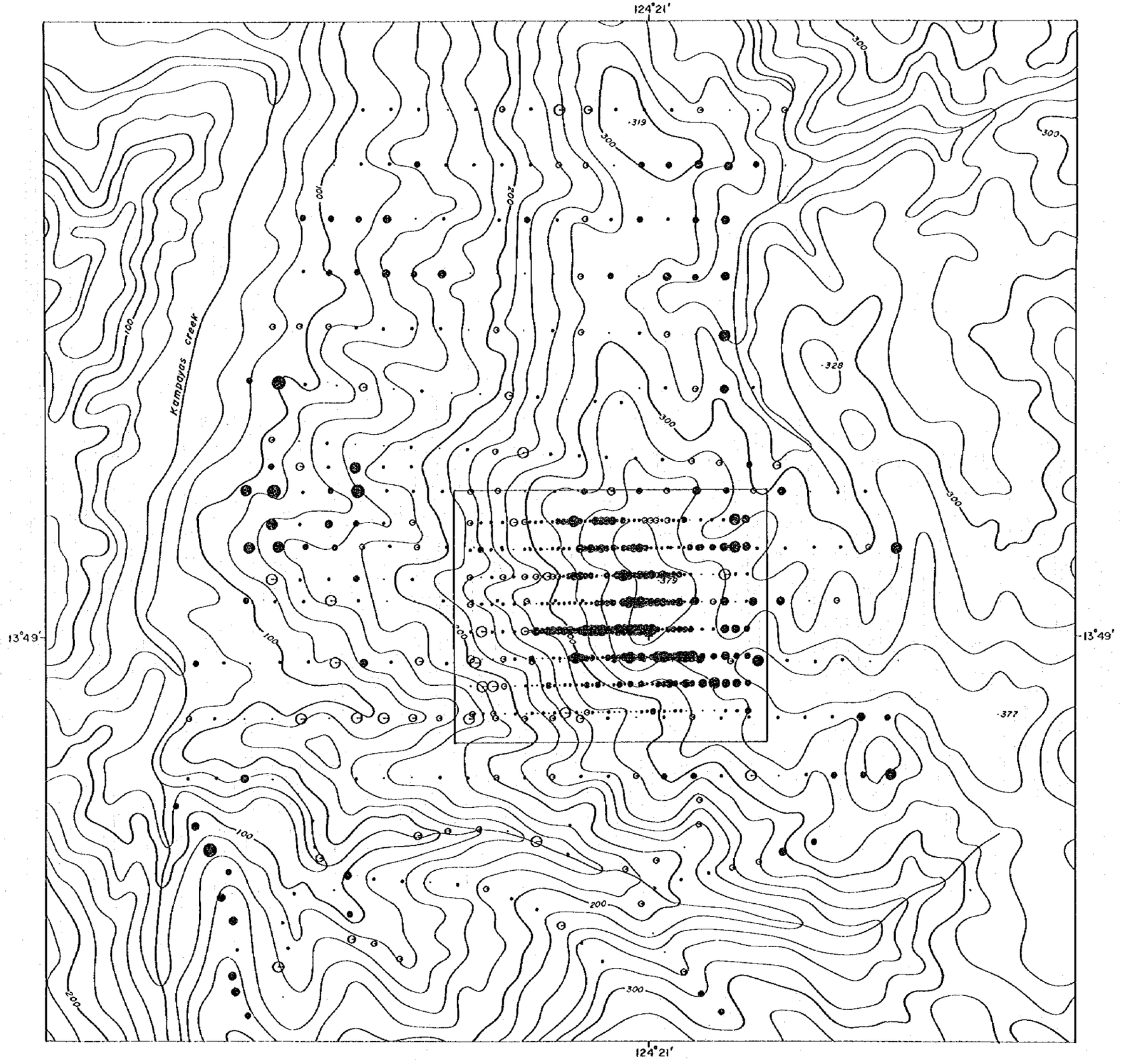

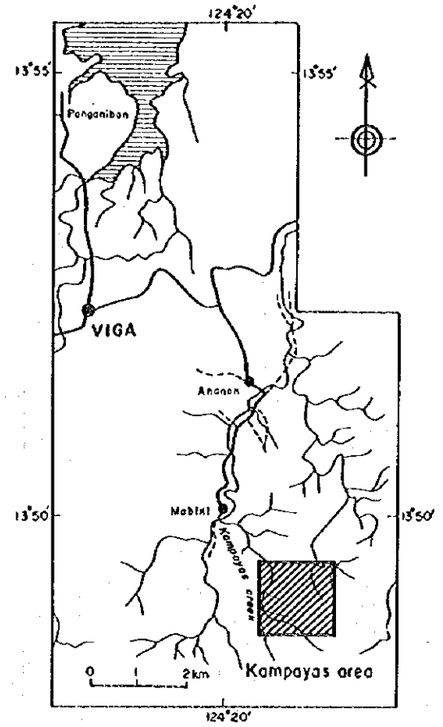

Z-01 (S-Fe-(-Zn)-(Pb))

- ⊖ : <-2.579
- ⊖ : <-1.834
- ⊖ : <-1.290
- • : <-0.845
- . : <-0.000
- • : < 0.645
- ◇ : < 1.290
- ● : < 1.834
- ● : < 2.579
- ● : > 2.579

0 100 200 300 400 500m

Fig. 9 Distribution of PCA Scores (1)

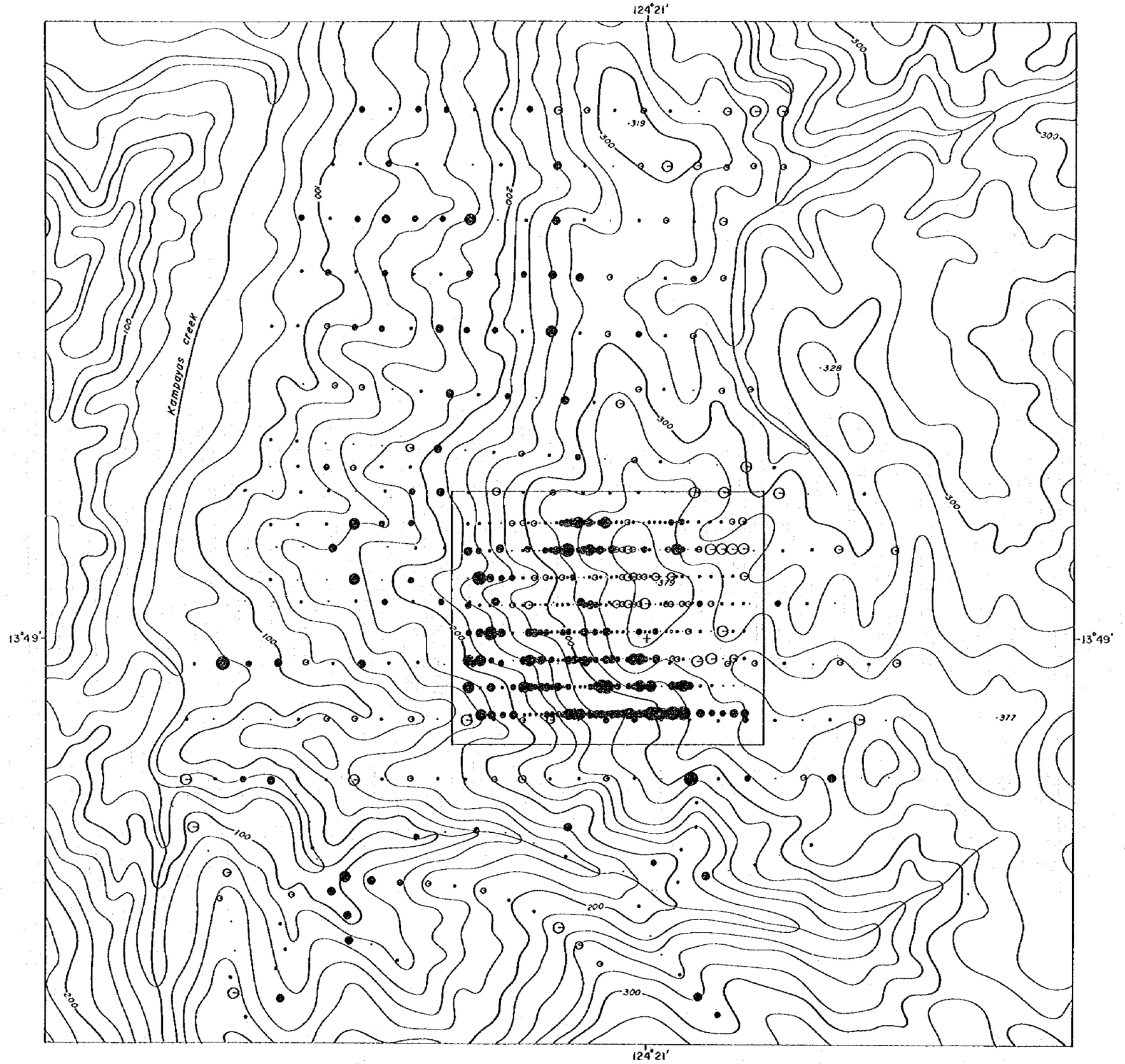

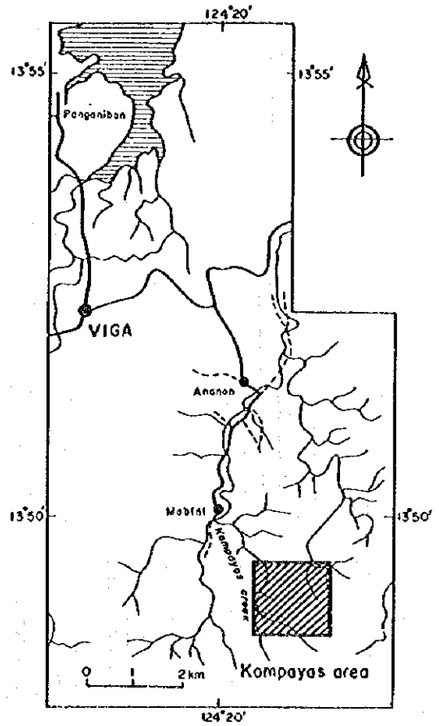

Z-02 (Cu-Zn-Pb)

: <-2.305

: <-1.728

: <-1.153

: <-0.578

: <-0.000

: < 0.578

: < 1.153

: < 1.728

: < 2.305

: > 2.305

0 100 200 300 400 500m

Fig. 9 Distribution of PCA Scores (2)

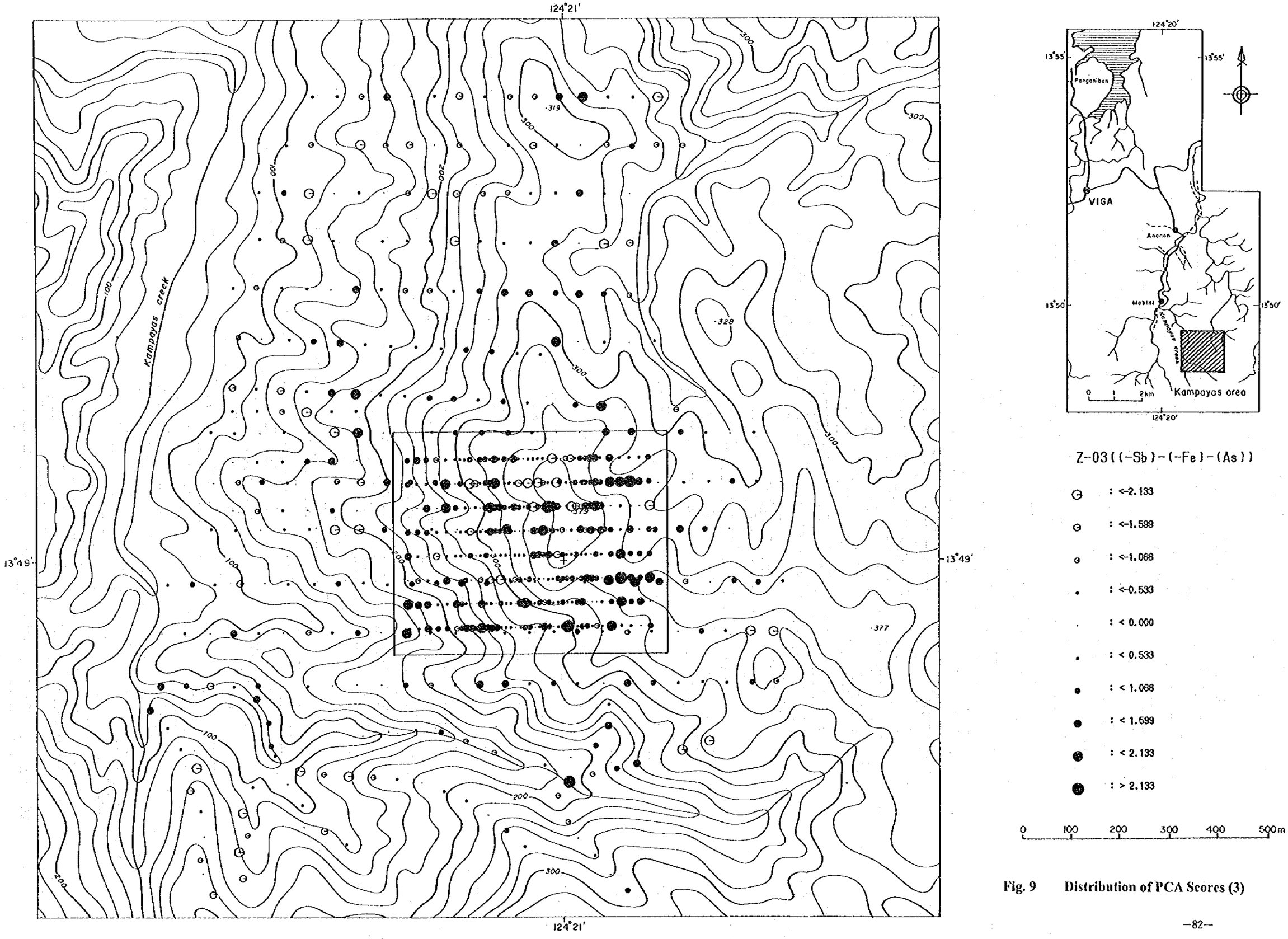

Z-03((-Sb)-(-Fe)-(As))

: <-2.133
: <-1.599
: <-1.066
: <-0.533
: < 0.000
: < 0.533
: < 1.066
: < 1.599
: < 2.133
: > 2.133

Fig. 9 Distribution of PCA Scores (3)

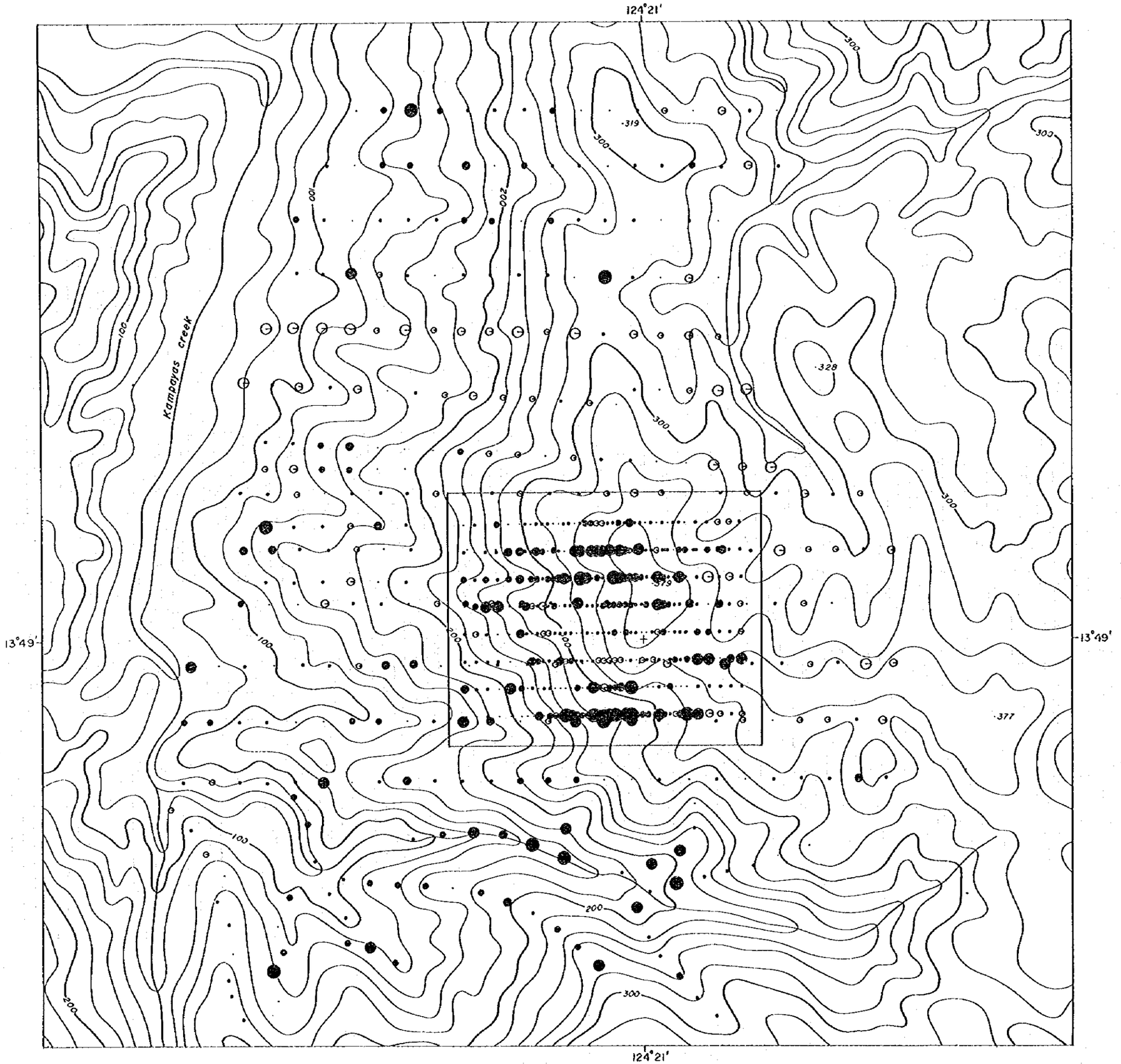

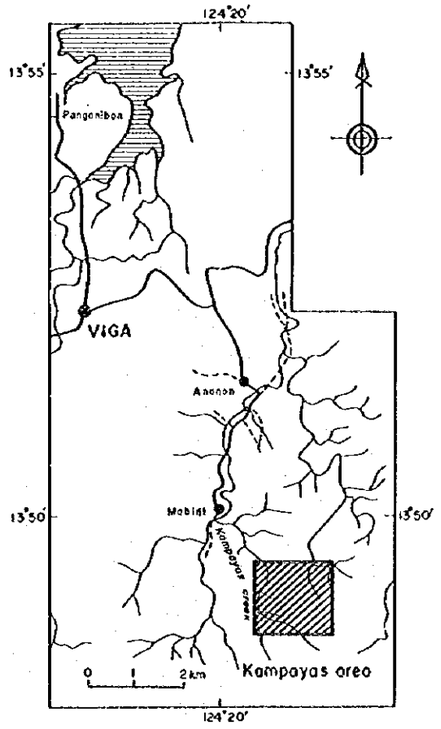

Z-04 (Au-(-As))

⊖	: <-2.037
⊖	: <-1.528
⊖	: <-1.019
•	: <-0.509
·	: <-0.000
•	: < 0.509
•	: < 1.019
•	: < 1.528
•	: < 2.037
•	: > 2.037

0 100 200 300 400 500m

Fig. 9 Distribution of PCA Scores (4)

Second principal component: This component has largely positive factor loadings of Cu, Pb and Zn, and suggests multiple base metal mineralization. High scores are distributed near the diorite body at the ridge around peak 379 m. Most of high scores exist at the western side of NNE-SSW oriented fault passing by the ridge around peak 379 m, while most of low scores are recognized at the eastern side of the fault.

Third principal component: This component has notably negative factor loading of Sb. It bears no meaning in the geology because most Sb show very low values, however.

Fourth principal component: This component has largely positive factor loading of Au and negative factor loading of As related to gold mineralization. High scores are distributed from the ridge around peak 379 m to the southern part. These high scores correspond to the Au high concentration areas and the areas are where numerous floats and outcrops of andesite porphyry and diorite are recognized.

The comprehensive map of the survey area was shown in Fig. 10.

2-1-7 Discussion

The variation of each element in Kampayas Area was controlled by the NNE-SSW oriented fault, by the diorite body at the ridge around peak 379 m and by the strongly silicified zone at the eastern part of Kampayas creek. The NNE-SSW oriented fault passing by the ridge of peak 379 m is believed to have served as channelways for the andesite porphyry and hydrothermal solutions.

Based on the results of geochemical survey, the highest gold potential areas are believed to be near the ridge of peak 379 m and at the intersection of the NNE-SSW and E-W oriented faults in the southern part of the detailed survey area. In particular, the site for forming a gold deposit is preferable at the above-mentioned intersection of the faults because the big quartz veins of about 20 cm (0.3 g/t Au) to 1 m in width and geochemical high gold anomalies are observed near the intersection.

It is highly possible that a promising gold mineralization exists at the relatively higher part (above the 200 m in altitude) in according to the following reasons; There are many soil samples yielding high values of 0.1 to 2.6 g/t Au at the ridge around peak 379 m and in the southern part. High gold anomalies (more than 10 g/t Au) were recognized by the stream sediments geochemical survey of the Second Phase Survey at the northern creek of the ridge. The quartz vein (KCR-08) of about 1 m in width at 200 m in altitude includes fluid inclusions

showing the temperature ranging from 203 to 285° C (Ave. 248° C) and has low value of 0.02 g/t Au. On the other hand, the quartz vein (KCR-09) of about 20 cm in width at 270 m in altitude shows fluid inclusions homogenizing at ranging from 189 to 262° C (Ave. 217° C) and has relatively high value of 0.3 g/t Au.

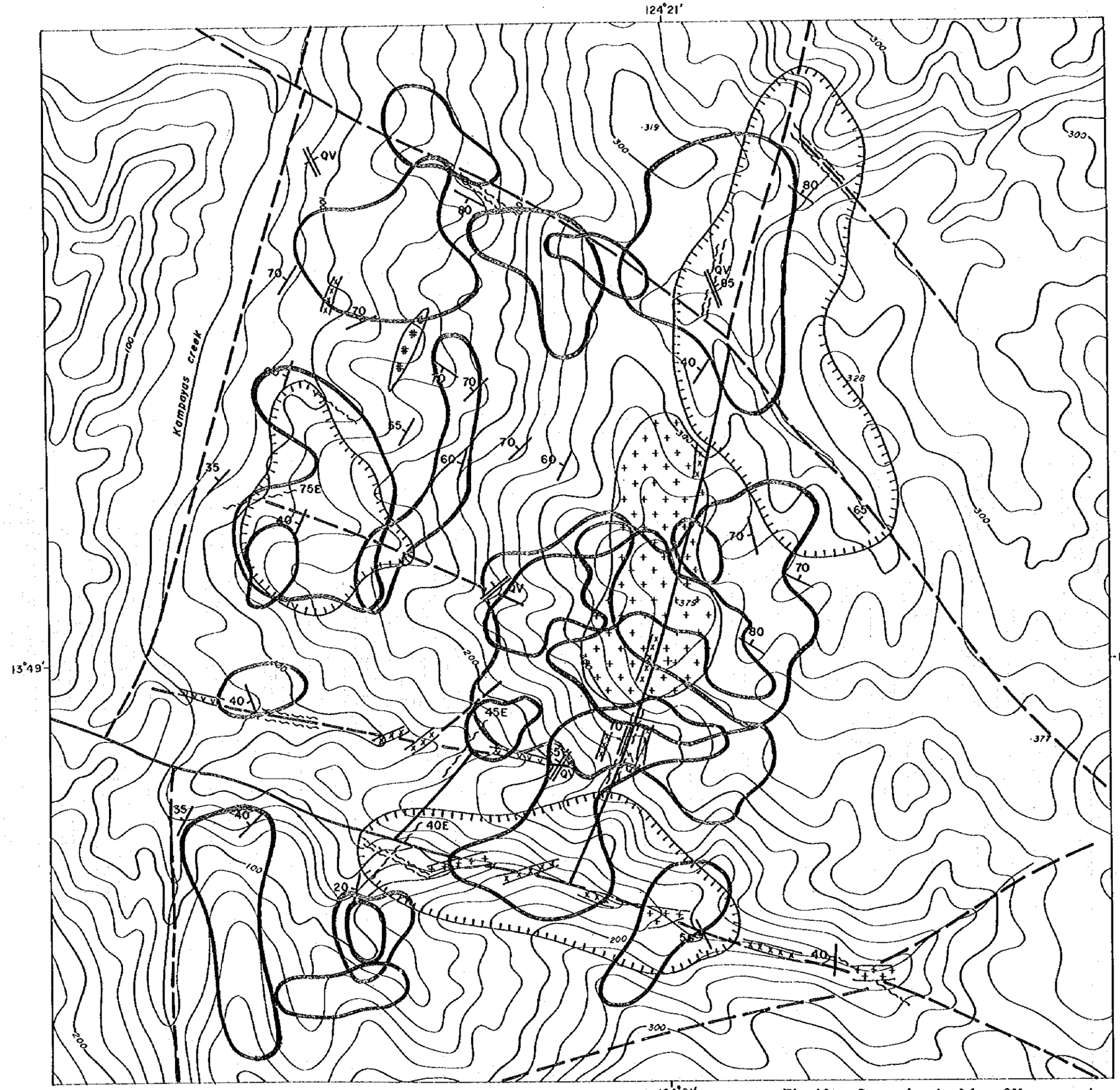

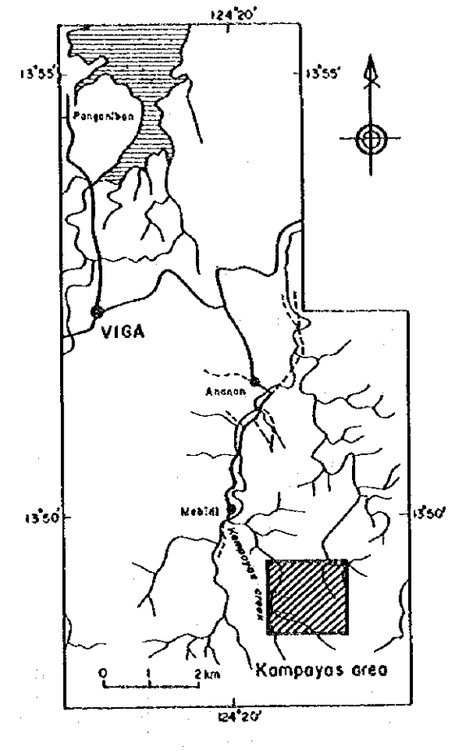

LEGEND

SYMBOLS ROCKS

- Sandstone/Lapilli tuff — Catanduanes Formation
- Andesite — Batalay Intrusives
- Andesite Porphyry — Batalay Intrusives
- Diorite — Batalay Intrusives
- Gabbro — Batalay Intrusives

GEOLOGIC STRUCTURE

- Fault (brocken line shows inferred F.)
- Sheared zone
- Strike and dip of strata
- Quartz vein >10cm
- Silicification & Pyritization

PCA of Soil Samples

High Score Anomaly

- Z - 01 (Fe, S)
- Z - 02 (Cu, Pb, Zn)
- Z - 04 (Au, - As)

0 100 200 300 400 500m

Fig. 10 Comprehensive Map of Kampayas Area

Chapter 3 Laboratory Works

3-1 Microscopic Observation

This analysis was carried out to verify the characteristics and occurrences of the rocks and the ores. The results were shown in Table 10 and Table 11.

The following observations were verified through microscopic observations:

(1) Though the greenschist is highly altered and the ratio of the rock forming minerals was different from each original rock, it is mainly composed of albite, quartz, chlorite, epidote, sericite and carbonates with subordinate amount of amphiboles, pyrite, magnetite and chalcopyrite as in samples taken from drilling cores of Carorongan Area. The metagabbro is mainly composed of albite, chlorite, epidote, carbonates and quartz with generally less amount of sericite, orthopyroxene, clinopyroxene, siderite, pyrite, magnetite, hematite and chalcopyrite.

(2) All the samples taken from drilling cores are altered. Strong pyritization, carbonatization and sericitization were observed in the thoroughly silicified metagabbro. Epidotization which was observed at deeper levels of the cores is characterized by the occurrence of magnetite.

(3) The ore samples (quartz veins) taken from the trenches are mainly composed of quartz with minor albite and sericite. The disseminations of pyrite or limonite are generally observable in the samples. The yellowish white colored gold minerals of about 5 μ m in diameter coexist with limonite in the sample of FT3-09.

(4) The sedimentary rocks in Kampayas Area were characterized by basic tuffaceous sandstone which are mainly composed of plagioclase and chlorite with minor amount of epidote and quartz.

(5) Numerous floats of altered diorite and relatively fresh andesite porphyry were recognized at the ridge around peak 379 m. The diorite is highly altered and mainly composed of chlorite, albite and quartz with small amount of epidote, sericite and calcite. The andesite porphyry is characterized by megacrystals of plagioclase, and composed of plagioclase, chlorite, epidote with small amount of quartz, amphiboles, calcite, pyrite and trace amount of clinopyroxene and chalcopyrite.

Table 10 Results of Microscopic Observation (Thin Sections)

No	Sample No.	Rock Type	Location	Rock forming mineral																Remarks
				Mon	Ch	Se	Ka	Ep	Ca	Pn	La	Ac	Q	Pl	Ab	Kf	Hb	Ap	Sh	Au	
1	JT3-09	silicified schist	Carorongan area		◎			○					○	△	○					△	
2	KCR-21	andesite porphyry	Kampayas area		○			○	○				△		◎	○	△			?	
3	KCR-32	fine sandstone	〃		◎			○					○		◎		△			·	
4	KER-20	medium sandstone	〃		◎			△					△	◎			△			○	graywacke
5	KFR-03	medium sandstone	〃		◎			○	△				△	◎			△	·		○	
6	KGR-01	andesite porphyry	〃		○			△		△			△	◎						○	
7	KJR-02	basic tuff	〃		◎	△		○	△	△			·	◎						△	
8	KJR-15	medium sandstone	〃		◎	△		△	○				○	◎					△	○	
9	KJR-32	coarse sandstone	〃		◎	△		△	○				△	◎						○	tuffaceous
10	KJR-35	micro diorite	〃		○	△		○					○	◎			◎				

[Symbols] ◎ : abundant ○ : common △ : small amount · : rare
Q:Quartz Mon:Montmorillonite Ch:Chlorite Se:Sericite Ka:Kaolinite Ep:Epidote Ca:Calcite Ab:Albite Kf:Potassium feldspar Pl:Plagioclase Hb:Hornblende
Au:Augite Ac:Actinolite La:Laumontite Pn:Prehnite Ap:Apatite Sh:Sphene

Table 11 Results of Microscopic Observation (Polished Thin Sections) (1)

No	Sample No.	Rock Type	Location	Opaque mineral											Rock forming mineral															Remarks
				Cl	Bo	Cp	Cv	Sp	Py	Pr	Mg	He	La	Ge	Ru	Mon	Ch	Se	Ka	Ep	Ca	Pn	La	Ac	Q	Pl	Ab	Kf	Hb	Ap	Sh	Au	
1	CCR-06	quartz vein	Carorongan area						○		○	△	△		·			○							◎	△	△			·			
2	CCR-15A	quartz vein	〃						◎			△	○	△											◎	○	◎						Au:310ppb, Pl rich, felsite ?
3	CCR-15B	quartz vein	〃						◎			·	○	△					△						◎	○	○			△			Mt→Py
4	CCR-17	quartz vein	〃			·			◎				△						?							○	◎						Au:800ppb, Mt→Py, Pl→Ab
5	JT4-50	quartz vein	〃										△												◎		△						
6	CJR-61	fine sandstone	〃										△				◎			○			?		○	○					△		basic tuffaceous
7	ET4-14	quartz vein	〃										△	△				△							◎								Au:150ppb
8	FT3-09	quartz vein	〃						△				○	△					?						◎			△					Au:58.8g/t, gold mineral: -
9	KCR-23	andesite porphyry	Kampayas area			○			○							·	○			△	△	△			△	◎			△				trach andesite?
10	KCR-28	andesite porphyry	〃			△			○		○	△				·	○			○	·				·	◎		·					
11	KCR-30	quartz vein	〃						△				△							◎					◎								
12	KCR-31	gabbro	〃			△			○							·	○			△					·	◎		△	◎				gabbro?
13	KCR-33	porphyrite	〃			○			○		·		△			-	○			△	·				△	◎		·	△			△	micro diorite?
14	KFR-04	andesite porphyry	〃										△				○			△					○	◎							
15	KGR-04	micro diorite	〃			△			○								○			△	△					◎			◎			△	
16	KJR-30	felsite	〃	·		○	·		○				△				○			○					◎	◎							
17	KJR-34	silt~fine sandstone	〃						○								◎								○	◎						△	fine grain pyrite

[Symbols] ◎ : abundant ○ : common △ : small amount · : rare

Cl:Chalcocite Bo:Bornite Cp:Chalcopyrite Cv:Covelline Sp:Sphalerite Py:Pyrite Pr:Pyrrhotite Mg:Magnetite He:Hematite La:Limonite Ge:Goethite Ru:Rutil
Q:Quartz Mon:Montmorillonite Ch:Chlorite Se:Sericite Ka:Kaolinite Ep:Epidote Ca:Calcite Ab:Albite Kf:Potassium feldspar Pl:Plagioclase Hb:Hornblende Au:Augite Ac:Actinolite La:Laumontite
Pn:Prehnite Ap:Apatite Sh:Sphene

Table 11 Results of Microscopic Observation (Polished Thin Sections) (2)

No	Sample No.	Rock Type	Location & drilling No.	Opaque mineral											Rock forming mineral														Remarks
				Cl	Bo	Cp	Cv	Sp	Py	Pr	Mg	He	Lm	Ge	Ru	Mon	Ch	Se	Ka	Ep	Ca	Pn	La	Ac	Q	Pl	Ab	Kf	Hb	Ap	Sh	Au	
18	3-15.75	strong altered rock	Cararongan area MJPC-3			△			◎			○				·	○	○			◎				△	△	◎						highly silicified,chl/sme : ·
19	3-18.85	silicified schist	〃 〃	·	△	·						○				·	○	○			◎				◎		△	·					clear schistosity
20	3-88.70	quartz- axinite vein	〃 〃			·											○				◎				◎								axinite :◎ , chl/sme : ·
21	4-22.20	metagabbro	〃 MJPC-4			○			○		○	△					◎	△		△	◎				◎	△	◎						
22	4-26.90	metagabbro	〃 〃			·					△	○				·	◎			○	○				○	○	○	·					
23	4-62.00	basic tuff breccia	〃 〃			·					○						○			◎	◎				△	○	○		△				
24	5-12.80	altered fine sandstone	〃 MJPC-5			△			△			◎					○	○			◎				○	△	◎						
25	5-26.40	silicified rock	〃 〃			△			◎		△	○					○				◎				△	△	◎						host rock :black shale?
26	5-27.85	silicified metagabbro	〃 〃			○		·	◎		△	○	○				△				◎				○	△	◎						strongly altered, Au:2.7g/t
27	5-33.15	metagabbro	〃 〃			○				?		○	○				◎	○			◎				△	◎	△						low Au :19ppb
28	5-40.45	altered rock	〃 〃			△			◎			◎	△				○	△			◎				○	△	◎						host rock :Gb or fss ?
29	5-41.45	altered rock	〃 〃			○			○		△	○					○	△			◎				◎	△	◎						host rock :metagabbro
30	5-44.95	shale~siltstone	〃 〃								◎	○					○	○		◎	○				○	△	○						magnetic
31	5-60.00	shale~siltstone	〃 〃			○						◎				·	○	◎			◎				◎	○	△						
32	5-74.20	basic lapilli tuff	〃 〃	·		·			·			○				·	◎	○		◎	○				○	△	◎		○		○		green biotite :△
33	5-119.1	pelitic schist	〃 〃		△						◎						○	○		◎	○				○	△	◎		△				green biotite :△ ,magnetic
34	6- 8.55	strong altered rock	〃 MJPC-6			·			○								△	◎			◎				△		◎						quartz poor
35	6-11.50	strong altered rock	〃 〃			△		·	◎			△					△	◎			◎				△		○	·					quartz poor, Au:0.5g/t
36	6-22.70	strong altered rock	〃 〃			△		·	◎			·					△	◎			◎				△		○						
37	6-27.50	shale~siltstone	〃 〃								△	○				·	◎	○			○				◎		○	·					

[Symbols] ◎ : abundant ○ : common △ : small amount · : rare

Cl:Chalcocite Bo:Bornite Cp:Chalcopyrite Cv:Covelline Sp:Sphalerite Py:Pyrite Pr:Pyrrhotite Mg:Magnetite He:Hematite Lm:Limonite Ge:Goethite Ru:Rutil
Q:Quartz Mon:Montmorillonite Ch:Chlorite Se:Sericite Ka:Kaolinite Ep:Epidote Ca:Carbonate Ab:Albite Kf:Potassium feldspar Pl:Plagioclase Hb:Hornblende Au:Augite Ac:Actinolite La:Laumontite
Pn:Prehnite Ap:Apatite Sh:Sphene

Table 11 Results of Microscopic Observation (Polished Thin Sections) (3)

No	Sample No.	Rock Type	Location & drilling No.		Opaque mineral											Rock forming mineral															Remarks
					Cl	Bo	Cp	Cv	Sp	Py	Pr	Mg	He	Lm	Ge	Ru	Mon	Ch	Se	Ka	Ep	Ca	Pn	La	Ac	Q	Pl	Ab	Kf	Hb	Ap	Sh	Au	
38	6-31.50	silicified rock	Cararongan area	MJPC-6						◎				△				△	○			◎				◎	·	◎						host rock :metagabbro
39	6-33.10	metagabbro	〃	〃			○							○			·	◎	△			○				○	○	◎						
40	7-48.75	metagabbro	〃	MJPC-7								○	○				·	◎	△		△	○				△	△	◎					△	low Au :3ppb
41	7-52.40	metagabbro	〃	〃			○					◎					·	◎	△		△	△				△	○	○						chilled margin of gabbro
42	8-99.55	metagabbro	〃	MJPC-8								○	○	△			·	◎	△			○				△		○					○	serpentine:△～○
43	9-58.85	silicified rock	〃	MJPC-9			△			○		△	△					△				◎				○	△	◎						host rock :m.sandstone?
44	9-60.50	silicified rock	〃	〃			△			○		△	○				·	△	△			◎				○		◎						
45	9-61.65	silicified rock	〃	〃			△			○		△	○				·	△	△			◎				○	◎							metagabbro?
46	9-67.50	metagabbro	〃	〃			·					△	○	○			·	◎	·			◎					○	○					△	Au :4ppb
47	9-69.30	silicified metagabbro	〃	〃			△		·	◎		△	△					△				◎				◎	○	○						Au :310ppb
48	12-44.50	metagabbro	〃	MJPC-12			○					◎	△				·	◎	△			○				△	◎	○					△	Au :6ppb
49	KFR-9-1	diorite	Kampayas area											△			·	◎			○	·			○	◎		◎	△					highly altered
50	KFR-9-2	andesite	〃											△			·	◎			○					△		◎	△					highly altered, trachytic
51	KFR-11	altered andesite	〃											△			?	◎								◎		○						
52	BC- 2	dolerite	〃			·						○					·	◎	○			△	△				◎						△	serpentine(antigorite) :△

[Symbols] ◎ : abundant ○ : common △ : small amount · : rare

Cl:Chalcocite Bo:Bornite Cp:Chalcopyrite Cv:Covelline Sp:Sphalerite Py:Pyrite Pr:Pyrrhotite Mg:Magnetite He:Hematite Lm:Limonite Ge:Goethite Ru:Rutil
Q:Quartz Mon:Montmorillonite Ch:Chlorite Se:Sericite Ka:Kaolinite Ep:Epidote Ca:Carbonate Ab:Albite Kf:Potassium feldspar Pl:Plagioclase Hb:Hornblende Au:Augite Ac:Actinolite La:Laumontite
Pn:Prehnite Ap:Apatite Sh:Sphene

3-2 X-ray Powder Diffraction Analysis

The analysis was carried out to verify the characteristics and occurrences of the rocks and the ores. The results were shown in Table 12.

Large amount of alteration minerals such as kaolinite, sericite, limonite and gibbsite occur on the surface of Carorongan Area because the rocks are affected by tropical weathering. However, it is highly possible that some portions of kaolinite and sericite were formed by the hydrothermal alteration related to gold mineralization.

From the drilling samples, the gold mineralization in Carorongan Area is characterized by silicification with strong cabonatization, sericitization and pyritization. Epidotization is generally recognizable around the silicified zone, especially at deeper levels. The following characteristics are very distinct regarding the occurrences of iron-bearing minerals and carbonates; the iron-bearing minerals are generally composed of pyrite while the carbonates are mainly composed of dolomite - ankerite series minerals in the high Au zone; whereas in the low Au zone the iron-bearing minerals are generally composed of epidote and magnetite, while the carbonates are mainly composed of calcite. Most of the chlorite is relatively recognizable in the low Au zone and hematite generally exists throughout cores.

In Kampayas Area, the andesite porphyry and diorite of the Batalay Intrusives have already been exposed and its occurrence is different from the ones in Carorongan Area. The characteristic of X-ray diffraction analysis is that potassium feldspar and amphiboles are often recognizable here.

Microdiorite at the ridge around peak 379 m is highly altered wherein the quartz stands out from the matrix and most of the plagioclases is altered to albite in the X-ray diffraction analysis. Secondary potassium feldspar also occurs.

The strongly silicified zone and quartz veins at the eastern part of Kampayas creek are mainly composed of quartz, epidote and pyrite.

Table 12 Results of X-ray Powder Diffraction Analysis (1)

Sample No.		Locality / Rock Type \ Alteration Mineral	Clay Mineral						The Others Mineral																
			Mon	Chl /Mon	Se /Mon	Chl	Se	Ka	Gi	Q	Ab	Bf	An	Cu	Ak	Py	Hb	Di	Ep	He	Pb	Mt	La	Az	Sl	Sp
1	KCR-02	Kampayas area ,silicified vein w=2~3cm								○	·								○				·			
2	KCR-03	〃 ,silicified vein w=10cm	·			·				●	○								○				○			
3	KCR-21	〃 ,diorite				○					○	○		△		·	△		△							
4	KCR-23	〃 ,porphyrite	·	·		○	·			△	●			△		·							·			
5	KCR-24	〃 ,diorite	·			●	·			△	●	△		·		·	△		·							
6	KCR-27	〃 ,schist				○				·	●			△									·			
7	KCR-28	〃 ,sandstone	·			△				·	●	·		·		·			△				·			
8	KCR-30	〃 ,Q.V.				·				◆						·			○				·			
9	KCR-31	〃 ,micro gabbro	·			○	·				●	△				·	○		△							
10	KCR-33	〃 ,sandstone	·	·		●	·			△	●	·		·		·			△				·			
11	KCR-36	〃 ,Q.V.								●	△			△					△				·			
12	KER-11	〃 ,Q.V. w=15cm				△	·			●	○	○				·							△	·		
13	KER-12	〃 ,silicified rock				○	△			●	○	△				·							△			
14	KFR-04	〃 ,porphyrite	·			△				○	●			·					△				·			
15	KGR-04	〃 ,diorite				○				○	●	△		·		·	○		△							
16	KJR-03	〃 ,	·			△		·		△	○	△							·				△			
17	KJR-32	〃 ,sandstone				○	·			·	○			○					·				△			
18	KJR-33	〃 ,weathered tuff	△			△	△	·		·	○			·					·				△			
19	KKR-9-1	〃 ,micro diorite	·			○				◆	●	△		·					·							
20	KKR-9-2	〃 ,andesite	·	·		○	·			◇	●	△							·							
21	BC- 2	〃 ,gabbro	·			△	△					·	○					△								△
22	OCR-02	Ceremongan area, Q.V. w=1~3cm					·		△	●	○												△			
23	OCR-10	〃 , Q.V. w=20cm				△				●	△								·				△			
24	OCR-15	〃 , Q.V. Py imp.								●	○					○							○			
25	OCR-17	〃 , Q.V. Py imp.								○	●												·			
26	CJR-63	〃 ,clay				·	·			○	●					·			·				○			
27	JT1-25	〃 (Trench No.1)							△	●													○			
28	JT3-09	〃 (Trench No.3),Q.V.							·	●													△			
29	JT3-08	〃 〃 ,schist				△	△	△	△	○	·								△							
30	JT4-16	〃 (Trench No.4),argillitic part	·			○	△	·		○	○	·											△			
31	JT4-51	〃 〃 ,clay		·	·	●	○				○	·														
32	GTS-02	〃 (Trench No.5),schist				·	△	○	△	○		·							△				○			
33	GTS-13	〃 〃 ,schist	·		·	○	○	△	△	●	△	·							△							
34	GTS-15	〃 〃 ,schist	·		·	○	○	△	△	◆		·							·							
35	GTS-22	〃 〃 ,schist			·	·	△	○		○									·				○		·	
36	GTS-25	〃 〃 ,schist	·				△	●		○									·				○			
37	GTS-35	〃 〃 ,schist	·				○	○	·	●		·							△				○			
38	GTS-41	〃 〃 ,schist					●	○	·	●		·							△				△			
39	JTS-58	〃 〃 ,weathered schist			·		○	○											·							
40	BTG-01	〃 (Trench No.6),Q.V.				·	△	△	·	●									△				○			

[Symbols] ● : abundant ○ : common △ : few · : rare

[Abbreviations] Mon:Montmorillonite Ch:Chlorite Se:Sericite Ka:Kaolinite Ph:Pyrrhotite Q :Quarts Ab:Albite Bf:K-feldspar An:Anorthite
Cu:Calcite Ep:Epidote Hb:Hornblende Mt:Magnetite He:Hematite Py:Pyrite Ak:Akerite Az:Azinite Sl:Sepiolite Gi:Gibbsite
Di:Diopside Sp:Serpentine La:Limonite

Table 12 Results of X-ray Powder Diffraction Analysis (2)

Sample No.		Locality / Rock Type \ Alteration Mineral	Clay Mineral						The Others Mineral																
			Mon	Chl/Mon	Se/Mon	Chl	Se	Ka	Gi	Q	Ab	Bf	An	Ca	Ak	Py	Hb	Di	Ep	Be	Ph	Mt	La	Ax	Sl	Sp
41	FI6-07	Cerorongan area(Trench No.6),Q.V.								●													○			
42	FI6-08	〃 〃 ,weathered schist					・	○	・	●										・			○			
43	FI6-11	〃 〃 ,quartz					・	○	・	●										・			○		・	
44	JT7-21	〃 (Trench No.7),Q.V. φ10×15cm							△	●													○			
45	JT9-38	〃 (Trench No.9),schist				●	○		○	・	△	・								△			●			
46	3-15.75	〃 (Drill hole No.3),gabbro	・	・		△	○			・	●			○	●	・										
47	3-18.85	〃 〃,gabbro~igneous rock	・			△	○			●	△	・		・	○					・						
48	3-88.70	〃 〃,Q.V. φ8cm		・		△	・			●	・	・		●										●		
49	4-22.20	〃 (Drill hole No.4),gabbro				△	・			●	●	・		・	●	・										
50	4-26.90	〃 〃,gabbro	・			●	・			○	○	・		△					・		・					
51	4-62.00	〃 〃,basic tuff breccia				△	・			・	○			●			△		△							
52	5- 6.50	〃 (Drill hole No.5),sandstone	・			●	○			●	△	・								・						
53	5-12.60	〃 〃,silicified rock				△	○			○	●			△	●	・										
54	5-26.40	〃 〃,silicified gabbro	・			○				△	●			・	●	・				・						
55	5-27.85	〃 〃,gabbro				△				○	●			・	●	△										
56	5-33.15	〃 〃,gabbro	・			○	△			○	●			○												
57	5-40.45	〃 〃,silicified gabbro				△	・			○	●			△	●	・										
58	5-41.45	〃 〃,silicified gabbro				・	・			○	●			△	●	・						・				
59	5-44.95	〃 〃,shale~sandstone				○	○			○	○			△		・			△							
60	5-60.00	〃 〃,shale	・	・	・	○	○			●	△			○	○					△						
61	5-74.20	〃 〃,basic tapilli tuff	・			●	・			○	●			△			△		△							
62	5-119.10	〃 〃,shale~sandstone	・	・	・	△	○			○	●			・		・	△		△						・	
63	6- 8.55	〃 (Drill hole No.6),silicified				・	○				●				●	・										
64	6-11.50	〃 〃,silicified rock				・	●				○	・			●	・										
65	6-22.70	〃 〃,silicified rock				・	○			・	○				●	△										
66	6-27.50	〃 〃,shale~sandstone	・			●	△			●	○	・		○						・						
67	6-31.50	〃 〃,silicified rock					△			●	●			・	●	・										
68	6-33.10	〃 〃,gabbro	・			●	△			○	○			○	・	・										
69	7-48.75	〃 (Drill hole No.7),gabbro	・	・		●	△			△	○			○	・	・										
70	7-52.48	〃 〃 ,gabbro	・			●	・		・	△	●			△								・				
71	8-19.70	〃 (Drill hole No.8),argillized					・	△		△	●									・						
72	8-93.55	〃 〃,gabbro	・	・		●	△			○	○			○	・	・					・					
73	9-20.10	〃 (Drill hole No.9)	・			・	○	・		●	△															
74	9-58.85	〃 〃,silicified part				・				○	●			・	●	・										
75	9-61.50	〃 〃,Q.V. φ30cm	・			△	△			○	○			△	●	・					・					
76	9-63.30	〃 〃				○	・			●	●			△	●	・										
77	9-67.50	〃 〃,gabbro	・	・		●	・			△	●			●		・					・					
78	9-69.30	〃 〃,silicified gabbro	・			△				・	●				●	△										
79	12-44.50	〃 (Drill hole No.12),gabbro	・			●	・			○	●			△		・					・	・				

{Symbols} ●:abundant ○:common △:few ・:rare

{Abbreviations} Mon:Montmorillonite Ch:Chlorite Se:Sericite Ka:Kaolinite Ph:Pyrrhotite Q:Quarts Ab:Albite Bf:K-Feldspar An:Anorthite
Ca:Calcite Ep:Epidote Hb:Hornblende Mt:Magnetite He:Hematite Py:Pyrite Ak:Ankerite Ax:Axinite Sl:Sepiolite Gi:Gibbsite
Di:Diopside Sp:Serpentine Li:Limonite

3-3 Homogenization Temperature of Fluid Inclusion

Most of the rocks are highly silicified and carbonized in the survey area. The homogenization temperature measurement of fluid inclusions was carried out to verify the relationship between the mineralization and the above-mentioned alteration. The results were shown in Table 13 and Fig. 11.

The quartz veins taken in the trenches have many impurities and are stained white. The vapor facies are not generally recognizable in the inclusions because of the very small sizes. The fluid inclusions which have 5 to 10 μm in diameter, though rarely exist, were used for the measurement. The homogenization temperatures of the fluid inclusions in the quartz veins taken from the trenches show a peak at around 200° C. Samples of FT3-03 (23.9 g/t Au) and FT3-09 (58.8 g/t) having high Au present the normal distribution with the peak falls at around 200 to 220° C.

The quartz veins taken from the drilling cores are classified into 3 types; the first type includes many impurities, the second type is relatively transparent and the third type shows veinlets having 3 to 5 mm in width. Generally, the first type is stained white and often includes fluid inclusions homogenizing at more than 300° C. The second type has many fluid inclusions having the peak at 250 to 300° C. The first and second types frequently have fluid inclusions showing bimodal peaks at around 180° C and 300° C. The third type has fluid inclusions formed in low temperature conditions at around 200° C.

In MJPC-5 where the strongest silicification is recognized, the samples were taken from several points from shallow to deep levels to determine the vertical variation of the homogenization temperatures. As a result, the fluid inclusions in all homogenized at around 350° C at the highest, however, the fluid inclusions in the samples taken at 60.45 m and 68.30 m yield peaks at the highest temperature side.

As compared with the fluid inclusions of samples taken from trenches, the ones from the drilling cores tend to show higher homogenization temperatures by about 50° C in the average.

In Kampayas Area, the quartz vein (KCR-08) of about 1 m in width at 200 m in altitude includes fluid inclusions showing the temperature ranging from 203 to 285° C (Ave. 248° C) and has low value of 0.02 g/t Au. On the other hand, the quartz vein (KCR-09) of

Table 13 Homogenization Temperature of Fluid Inclusions

Sample No.		Tested mineral	Result	Count No	Avg.(℃)	Homogenization temp.(℃)
1	KCR-08	Quartz	measured	6	248.2	203.0~285.0
2	KCR-09	Milky Quartz	measured	8	216.8	189.0~262.0
3	KCR-15	Milky Quartz	measured	9	241.3	151.0~296.0
4	KCR-22	Quartz	measured	17	182.8	160.0~207.0
5	KCR-30	Quartz	measured	8	184.5	139.0~233.0
6	KER-14	Quartz	measured	7	147.9	137.0~159.0
7	CCR-06	Milky Quartz	measured	14	193.0	138.0~230.0
8	CCR-07	Quartz	measured	4	198.5	166.0~240.0
9	CCR-10	Milky Quartz	measured	7	147.9	137.0~159.0
10	CCR-15	Quartz	measured	10	241.3	180.0~271.0
11	GT1-02	Quartz	measured	7	262.3	180.0~333.0
12	ET2-04	Milky Quartz	measured	11	208.7	135.0~273.0
13	JT2-34	Milky Quartz	measured	6	214.5	189.0~233.0
14	FT3-03	Milky Quartz	measured	21	211.8	168.0~285.0
15	FT3-09	Milky Quartz	measured	8	204.0	182.0~225.0
16	ET4-14	Milky Quartz	measured	8	208.1	150.0~244.0
17	JT4-50	Quartz	measured	10	218.7	186.0~273.0
18	JT4-52	Quartz	measured	5	249.4	224.0~261.0
19	GT5-01	Milky Quartz	measured	29	218.6	180.0~295.0
20	GT5-09	Quartz	measured	24	203.5	170.0~262.0
21	JT5-57	Quartz	measured	38	200.4	120.0~309.0
22	FT6-16	Quartz	measured	10	233.9	179.0~279.0
23	3-20.70	Quartz	measured	22	271.9	151.0~365.0
24	5-12.90	Milky Quartz	measured	20	218.8	122.0~344.0
25	5-27.95	Milky Quartz	no meas.			
26	5-31.75	Milky Quartz	measured	21	258.3	151.0~354.0
27	5-40.40	Milky Quartz	measured	13	227.9	169.0~289.0
28	5-60.45	Milky Quartz	measured	17	226.8	135.0~338.0
29	5-68.30	Milky Quartz	measured	15	271.7	182.0~310.0
30	5-105.00	Milky Quartz	measured	20	208.6	109.0~343.0
31	6-24.50	Quartz	measured	22	254.4	185.0~350.0
32	6-33.45	Quartz Veinlets	measured	11	180.0	132.0~204.0
33	6-40.60	Quartz	measured	27	250.3	107.0~365.0
34	6-60.45	Quartz	measured	19	186.3	151.0~231.0
35	6-85.00	Quartz Veinlets	measured	12	201.3	160.0~217.0
36	6-85.00	Calcite	measured	6	185.0	164.0~203.0
37	6-95.30	Milky Quartz	measured	14	228.1	169.0~357.0
38	9-60.50	Quartz Veinlets	measured	7	224.6	133.0~277.0
39	9-61.60	Quartz	no meas.			
40	9-85.70	Milky Quartz	measured	21	270.4	164.0~335.0

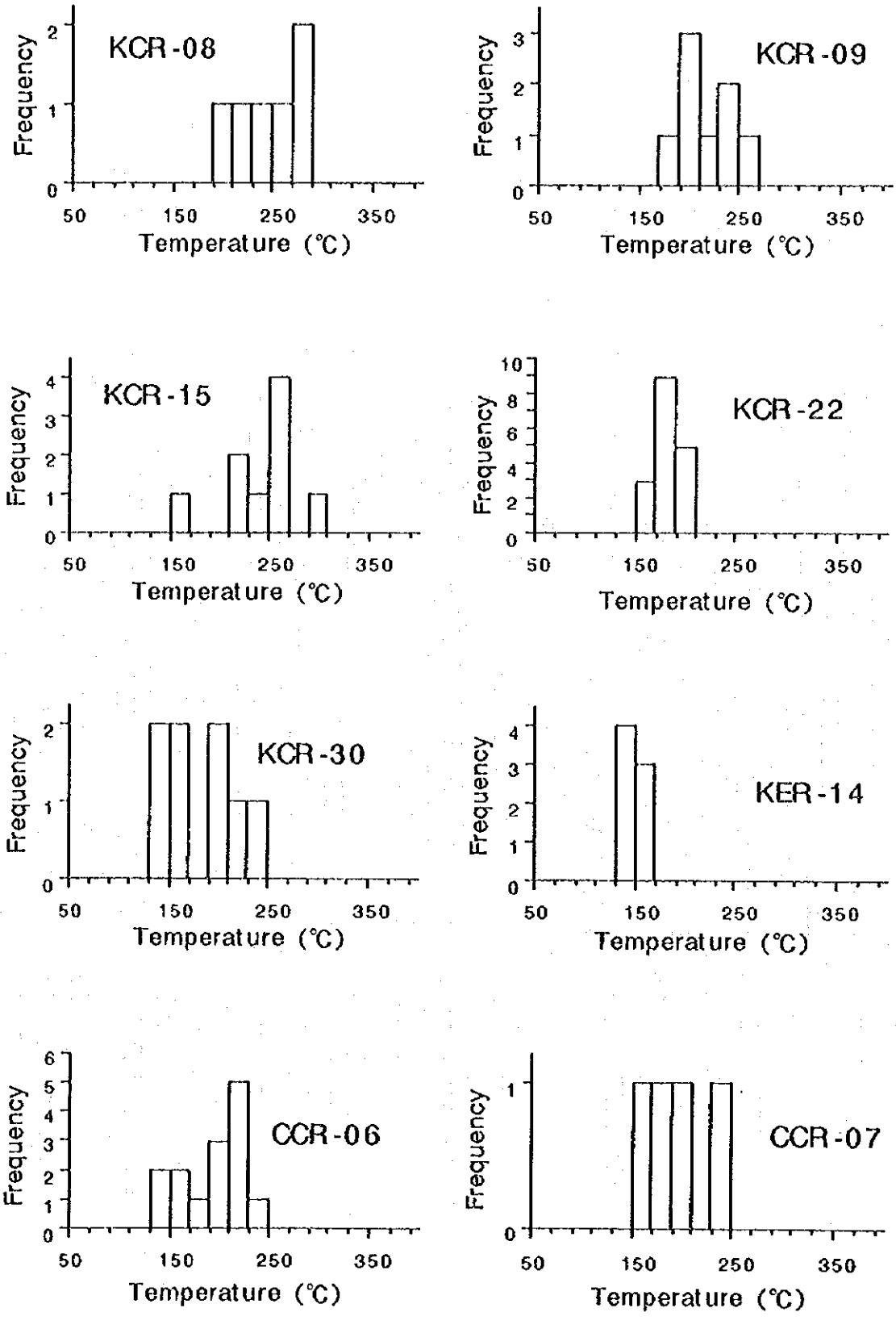

Fig. 11 Frequency Distribution of Homogenization Temperature (1)

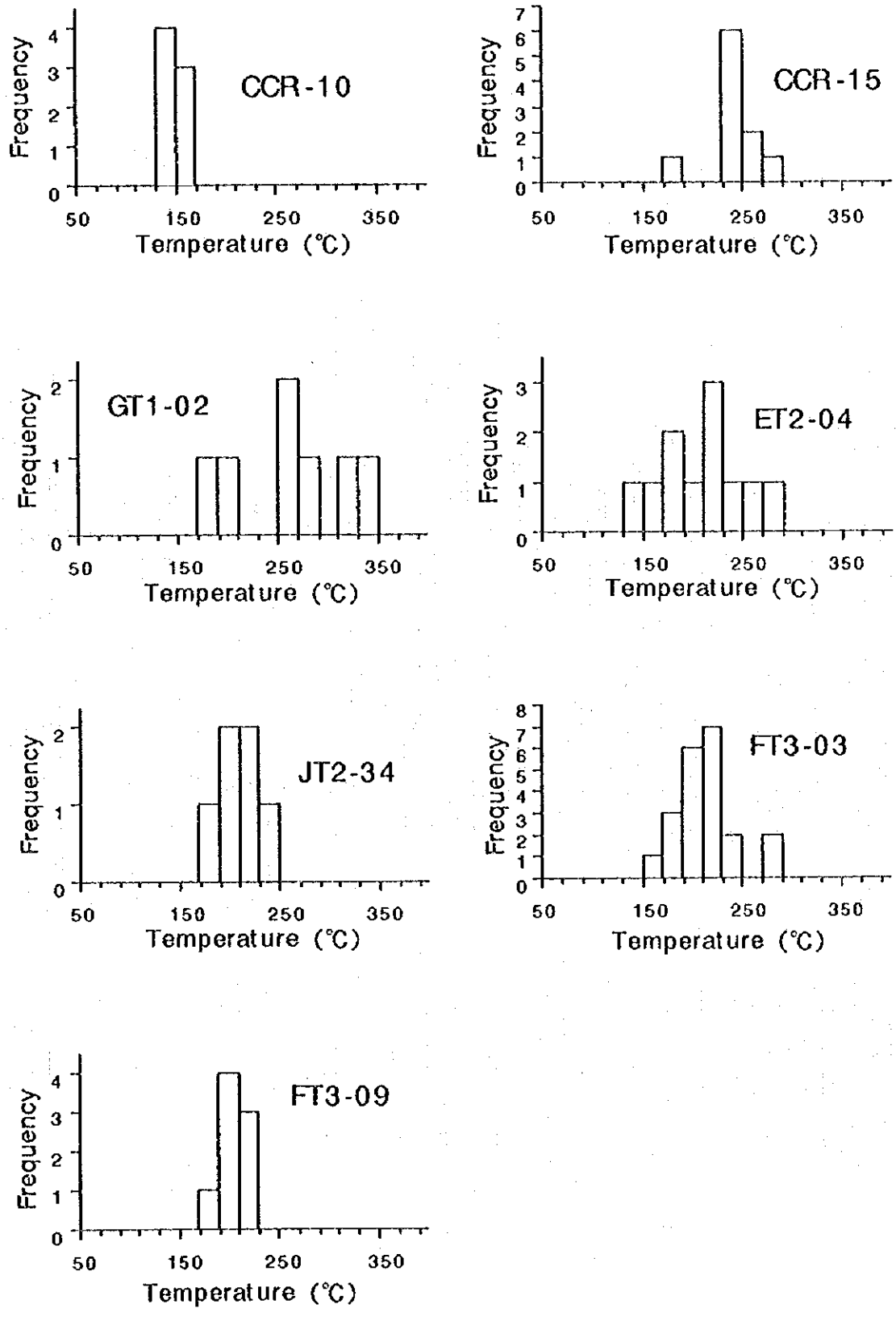

Fig. 11 Frequency Distribution of Homogenization Temperature (2)

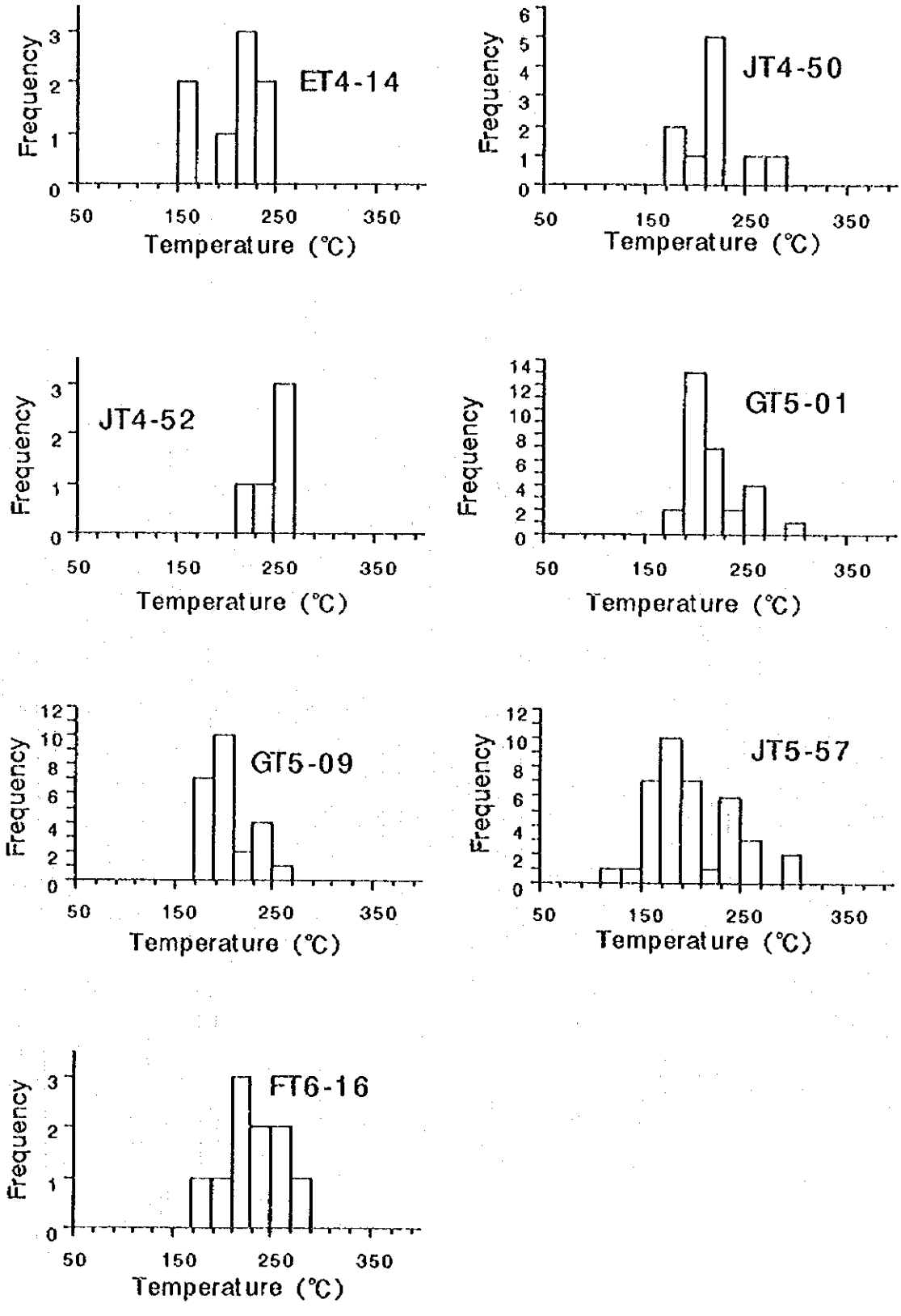

Fig. 11 Frequency Distribution of Homogenization Temperature (3)

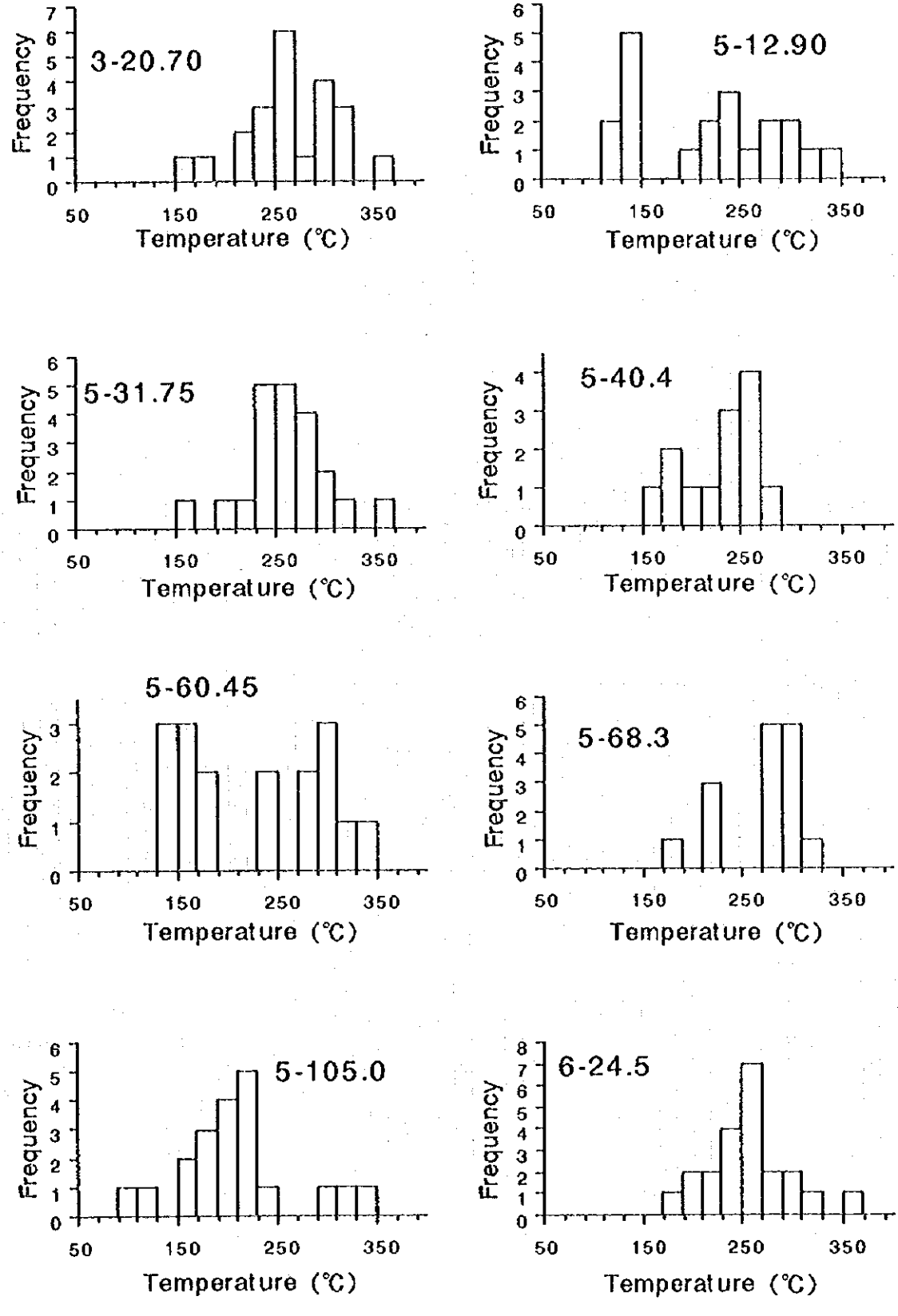

Fig. 11 Frequency Distribution of Homogenization Temperature (4)

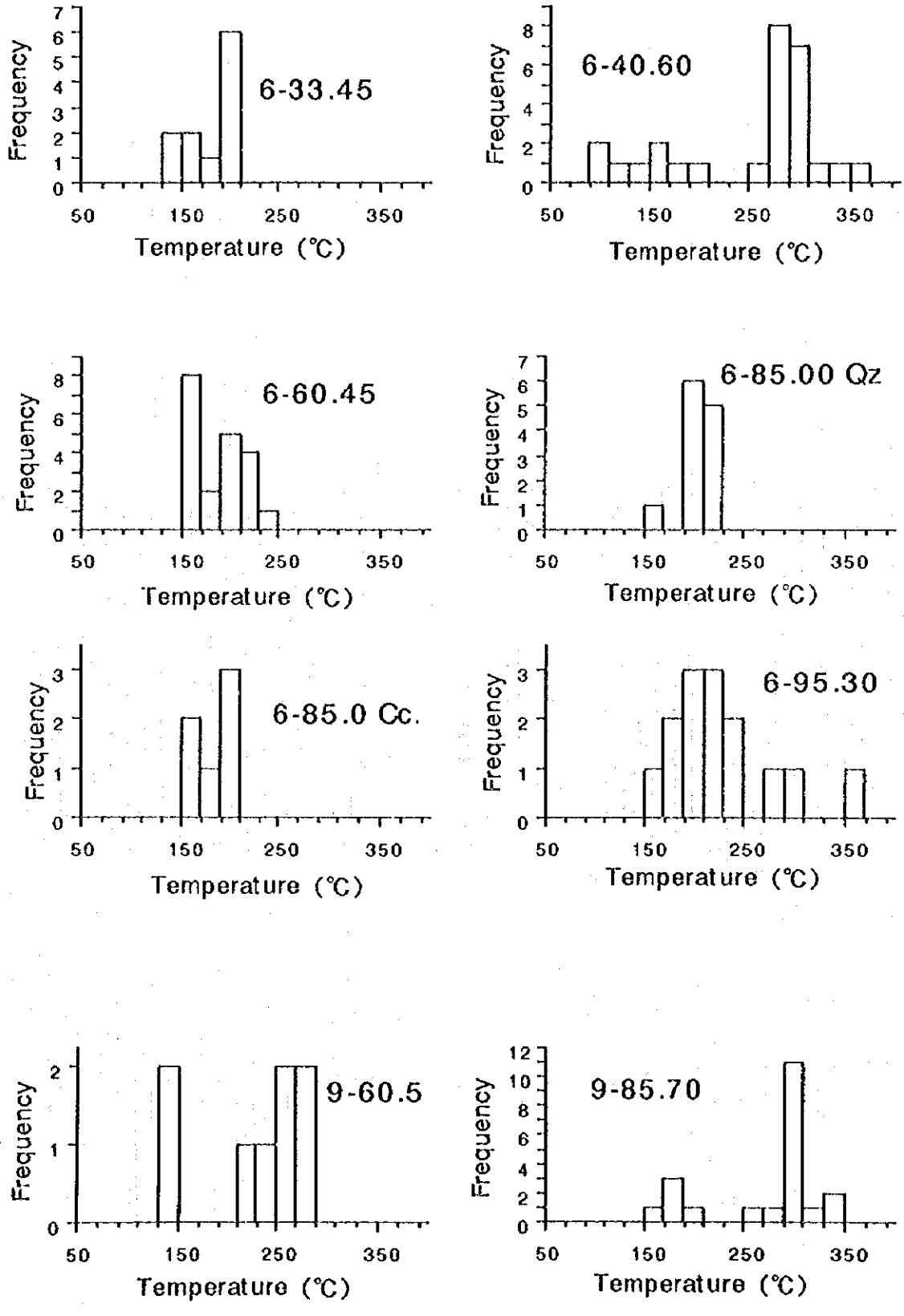

Fig. 11 Frequency Distribution of Homogenization Temperature (5)

about 20 cm in width at 270 m in altitude shows fluid inclusions homogenizing at ranging from 189 to 262° C (Ave. 217° C) and has relatively high value of 0.3 g/t Au. The soil samples taken near the latter quartz vein show high Au anomalies. Generally, quartz - epidote veins such as KCR-22 and KCR-30 have fluid inclusions formed in low temperature conditions at around 200° C.

3-4 K-Ar Dating

Age measurement by K-Ar method was made on three samples taken in Kampayas Area.

The samples were those of andesite porphyry (KCR-21), microgabbro (KCR-31) and microdiorite (KGR-04).

The constants were, according to Steiger and Jaeger(1977), set as follows:

$$\lambda e = 0.581 \times 10^{-10}/Y, \quad \lambda \beta = 4.962 \times 10^{-10}/Y$$

The existence rate of ^{40}K in K was set at $^{40}K/K = 0.01167$ atom %. The estimation of measurement errors was based on Nagao et al. (1984). The results were shown in Table 14.

The results of the age measurement revealed ages ranging from 26.7±0.6 Ma to 33.6 ±2.1 Ma. Those ages indicating the activity of Batalay Intrusives correspond to middle to late period of the Eocene. Based on these results, at least, the main mineralization in the Kampayas Area is interpreted to have occurred due to the hydrothermal activity related to Batalay Intrusives.

3-5 EPMA Analysis

The analysis was carried out to verify the compositions of carbonates related to the gold mineralization in Carorongan Area. The results were shown in Table 15.

In drill hole MJPC-5, most of the carbonates in the sample (5-27.85 m) yielding maximum Au value of 2.7 g/t are composed of dolomite with high Fe content, while the carbonates in the sample (5-33.15 m) yielding low Au value of 0.019 g/t are composed only of calcite. In drill hole MJPC-9, the carbonates in the sample (9-69.30 m) yielding high Au value of 0.31 g/t are also mainly composed of dolomite or ankerite, while the carbonates in the sample (9-67.50 m) yielding low Au value of 0.004 g/t are composed only of calcite. In the sample (7-48.75 m) taken from hole MJPC-7, where gold mineralization is not recognized,

Table 14 Results of K-Ar Dating

Sample No.	Rock Type	Sample Locality (latitude , longitude)	POTASSIUM (K wt%)	Rad. ^{40}Ar (10^{-6}cc/g)	K-Ar AGE (Ma)	AIR CONT. (%)	Average of K-Ar Age (Ma)
KCR-21	Porphyrite	Kampayas creek (N 13° 48′ 56″, E 124° 20′ 59″)	2.19±0.04	227±3.0	26.5±0.6	11.3	26.7±0.6
				229±3.0	26.8±0.6	11.9	
KCR-31	Gabbro	East of Kampayas creek (N 13° 49′ 52″, E 124° 20′ 59″)	0.68±0.04	89.5±1.3	33.8±2.1	26.5	33.6±2.1
				88.4±1.4	33.4±2.1	23.3	
KGR-04	Diorite	Kampayas creek (N 13° 48′ 15″, E 124° 21′ 00″)	0.91±0.06	109±2.0	30.5±1.9	19.7	30.2±1.8
				106±2.0	29.8±1.8	19.2	

* Dating was done on bulk samples by Mitsubishi Material Co.,Ltd. Central Laboratory.
* Decay Constant (after Steiger and Jaeger, 1977):
  $\lambda e = 0.581 \times 10^{-10}/Y$
  $\lambda \beta = 4.962 \times 10^{-10}/Y$
* ^{40}K content in K : $^{40}K/K = 0.01167$ atom %
* Error estimation was done after Nagao et al. (1984)

Table 15 Chemical Compositions of Carbonates

Sample Number	5-27.85m	5-27.85m	5-33.15m	5-33.15m	7-48.75m	7-48.75m
Sample Type	Dolomite	Dolomite	Calcite	Calcite	Calcite	Calcite
Weight Percent						
CaO	28.77	29.22	54.83	55.25	54.50	53.05
MgO	9.69	10.95	0.10	0.22	0.44	0.38
FeO	15.88	13.32	0.00	0.31	0.35	0.93
MnO	0.00	1.43	0.71	0.19	0.57	0.38
CO2*	42.89	43.94	43.59	43.90	43.82	42.86
Total	97.23	98.86	99.23	99.87	99.68	97.60
Atomic Ratio(CO3=1or2)						
Ca	1.053	1.044	0.987	0.988	0.976	0.971
Mg	0.493	0.544	0.003	0.005	0.011	0.010
Fe	0.454	0.371	0.000	0.004	0.005	0.013
Mn	0.000	0.040	0.010	0.003	0.008	0.006
CO3	2.000	2.000	1.000	1.000	1.000	1.000
Total	4.000	3.999	2.000	2.000	2.000	2.000

Sample Number	9-67.50m	9-67.50m	9-69.30m	9-69.30m	KCR-23	KCR-23
Sample Type	Calcite	Calcite	Dolomite	Dolomite	Calcite	Calcite
Weight Percent						
CaO	54.17	53.64	29.07	27.22	54.90	56.65
MgO	0.46	0.58	10.53	10.06	0.00	0.08
FeO	0.86	0.73	15.57	17.94	0.00	0.21
MnO	0.43	1.02	0.80	0.60	0.00	0.00
CO2*	43.80	43.81	44.35	43.71	43.09	44.67
Total	99.72	99.78	100.32	99.53	97.99	101.61
mic Ratio(CO3=1or2)						
Ca	0.971	0.961	1.029	0.977	1.000	0.995
Mg	0.011	0.014	0.519	0.503	0.000	0.002
Fe	0.012	0.010	0.430	0.503	0.000	0.003
Mn	0.006	0.014	0.022	0.017	0.000	0.000
CO3	1.000	1.000	2.000	2.000	1.000	1.000
Total	2.000	1.999	4.000	4.000	2.000	2.000

CO2*:Weight Percent calculated by Difference.

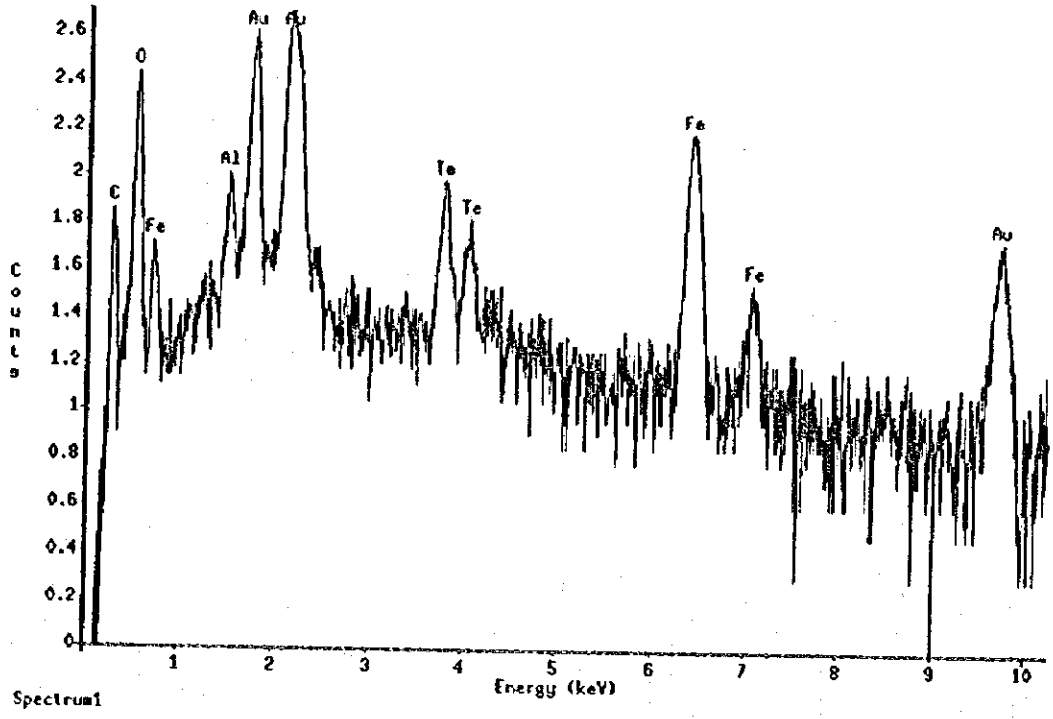

Colvan	: JXA-733,Pioneer		
Take-off angle	: 40	Accelerating voltage	: 20
Acquisition type	: eds	Magnification	: 1000
Creation time	: 95/10/30 16:45	Charge	: 15
Livetime	: 100	Beam current	: 0.15
Deadtime	: 30.758	Beam spot size	: 0
Channels	: 1024	Beam location	: 0.442247,0.363126
Channel width	: 10	Working distence	: 11
Detector type	: Silicon/Lithium	Stage X	: 0
Window type	: norvar	Stage Y	: 0
Window thickness	: 0.3	Stage Z	: 0
Coating material	: Al	Stage tilt	: 0
Coating thickness	: 0.04	Stage rotation	: 0
Contact material	: Au	Contamination material	: none
Contact thickness	: 0.02	Contamination thickness	: 0
Crystal thickness	: 3		

File name :

Notes:

Mon Oct 30 16:42:36 1995

Livetime : 16.5 Sec.
Technique: Least Squares Fit

Elements Present:
C (6), O (8), Si(14), Mo(41), Fe(26)

Energy	Intensity	Element
0.272	87	C Ka

Fig. 12 Chart of Qualitative Analysis for Gold Mineral

most of the carbonates are calcite. It is very interesting that the main species of carbonates change depending on the Au concentration even spatially close samples or within the same drill hole.

Yellowish white colored gold minerals of 5 μ m in diameter were recognized in the sample (FT3-09) taken from a trench. Qualitative analysis was carried out for gold minerals. Though the elements of Au, Te, Fe, Al and O shown in Fig. 12 were detected in spite of the smallness in size of the grains and the gold mineral was not separated from limonite, gold is believed to occur as Au-Te minerals.

3-6 Chemistry of Rocks and Ores

The igneous rocks distributed in the survey area are metagabbro, basalt and dolerite of the Cretaceous ages, and andesite porphyry and diorite of the Batalay Intrusives. In this survey the representative samples of these rocks were subjected to chemical analysis of major composition, ore (trace) elements and rare earth elements (REE). For the ore element analysis, 11 elements, Au, Ag, As, Cu, Hg, Mo, Pb, S, Sb, Zn and Fe, were detected for analysis. For the REE analysis, 10 elements, Ce, Eu, La, Lu, Nd, Sm, Tb, Th, U and Yb, were detected for analysis.

ICP-AES method was applied for the assay of the principal oxide components and minor elements, however FeO was assayed by titration method; gold by the neutron radioactivation analysis, and sulfur by the high frequency furnace combustion method.

The detection limits are 1ppb for Au, 0.2 ppm for Ag, 2ppm for As, Pb and Zn, 1 ppm for Cu and Mo, 0.001 % for S, and 0.01 % for principal component oxides.

3-6-1 Major Composition

The principal chemical compositions and the norm composition of igneous rocks were shown in Table 16. TAS (Fig. 13), Harker (Fig. 14), ACF (Fig. 15) and AFM (Fig. 16) diagrams were used in data analysis.

The rock type numbers 1, 2, 3 and 4 represent metagabbro, dolerite, gabbro, Batalay Intrusives, respectively.

The sandstone and greenschist have been excluded for petrologic discussion because the rock is clastic in nature as it was observed to contain rounded granules of basalt under the

microscope.

Batalay Intrusives: Drummond and Defant (1990), Defant and Drumond (1990), Defant et al. (1990) mentioned that the island arc rocks (andesite, dacite, rhyolite) formed by subduction activity are characterized by $SiO_2 \geqq 56$ %, $Al_2O_3 > 15$ %, and $MgO < 3$ %. According to David Jr. (1994), the SiO_2 content of Batalay Intrusives ranges from 59 to 69 %.

However, most of the rocks in Kampayas Area show $SiO_2 < 56$ %, $MgO > 3$ % and are different from the normal principal composition of Batalay Intrusives.

The samples KCR-21 and KCR-23 exhibit porphyritic texture through microscopic observations and are inferred to be andesite porphyry. However, the rock fall within the field of basaltic trachyandesite in TAS diagram and has the characteristics of alkaline rock series in X-ray diffraction analysis. The other samples are highly altered and have poor content of SiO_2 compared with the normal Batalay Intrusives. These rocks, however, are believed to have the characteristics of calc-alkaline rock series.

Dolerite: The sample BC-2 taken from non mineralized area in the western part of Kampayas Area contains 46.89 % SiO_2, 19.36 % Al_2O_3, 4.01 % MgO as its principal composition. In TAS diagram, the rock is in the field of trachybasalt. Because the rock shows medium grain size and holocrystalline texture through microscopic observation, the rock is inferred to be dolerite.

Gabbro: The sample KCR-31 contains 49.30 % SiO_2, 17.40 % Al_2O_3 and 5.99 % MgO. In TAS diagram, the rock plots near the boundary between trachybasalt and basalt. Because the rock shows holocrystalline texture in the microscopic observation, these rocks are inferred to be gabbro.

Metagabbro: These rocks are the only igneous rock in Carorongan Area. Because the rocks have strong schistosity similar to greenschist, the rocks were ascribed to as metagabbro in this survey. These rocks yield SiO_2 content ranging from 41.96 to 50.75 % by weight. In TAS diagram, the rocks are in the field ranging from tephrite to trachybasalt. Because these rocks possess medium to coarse grain and holocrystalline texture through microscopic observation, it is inferred to be gabbro. These rocks are different from the normal gabbro because they are poor Mg and very rich in Fe, however.

3-6-2 Ore Elements

The analysis was carried out to confirm the potential contents of each ore element in the basements and consider the influence of soil.

Appendix-1 shows the results of analysis. In calculating the mean values, for samples whose values were below the detection limits, the values of the half of the detection limit were used. As the values of Carorongan Area already have been mentioned in the other sections, this discussion only mentions about the values of Kampayas Area. Sampling locations of rocks in Kampayas Area were shown in Appendix-6.

The contents of most of the elements such as Ag, As, Hg, Mo, Pb, and Sb are generally low. As to the Cu, the andesite porphyry (KCR-23) yields maximum values of 0.038 %, however, most of the values of Cu are similar to the Clarke number. The values of Zn are about the same as the Clarke number. The values of Fe reflect the characteristics of each lithofacies. The values of sulfur tend to increase in the silicified and pyritized rocks.

As to the Au, unaltered to weakly altered rocks possesses values several times in comparison with the Clarke number, while the strongly altered rocks are in dozens times in comparison with the Clarke number. The silicified rocks with large amount of quartz veins and the quartz vein itself frequently contain values of 0.1 to 0.3 g/t Au. In Kampayas Area, the maximum Au value is detected in a quartz vein of about 20 cm in width along the NE-SW oriented fault passing by the ridge of peak 379 m. The value is 0.3 g/t Au.

3-6-3 Rare Earth Elements

Rare earth element analysis was conducted on 12 representative samples to compare with the previous data. The results of the analysis were shown in Table 17. Also the analytical values were standardized based on chondrite composition (Thompson et al., 1984, but only Eu according to Taylor and McLennan, 1985) and was shown in Fig. 17, REE pattern diagram.

Based on Fig.17, dolerite and gabbro in Kampayas Area and metagabbro in Carorongan Area differ to some extent in content but indicate the same flat pattern. All the patterns in this survey are slightly different from a REE pattern of typical island arc.

Table 16 Chemical and Normative Compositions of Rocks

SAMPLE No.	KKR-04	KGR-04	KGR-21	KGR-23	KGR-31	KKR-9-1	KKR-9-2	BC-2	3-18.85	5-27.85	5-33.15	5-44.95	5-60.00	5-74.20	7-48.75	9-67.50	12-44.50
ROCK TYPE	4	4	4	4	3	4	4	2			1				1	1	1
ROCK NAME	And. Po	Diorite	And. Po	And. Po	Gabbro	Diorite	Andesite	Dolerite	Sili. schist	Sili. gabbro	Metagabbro	Shale	Shale	Lp. tf.	Metagabbro	Metagabbro	Metagabbro
SiO2	51.48	53.57	53.01	54.09	49.30	57.88	56.92	46.89	46.89	46.54	41.96	51.53	44.22	48.19	46.81	44.68	50.75
TiO2	0.67	0.74	0.79	0.71	1.13	0.78	0.89	0.92	0.91	1.13	1.30	0.87	0.98	0.84	1.05	1.07	1.46
Al2O3	19.58	17.35	17.54	19.66	17.40	17.94	18.71	19.36	15.40	10.02	17.02	16.26	16.32	16.91	18.51	16.95	14.69
Fe2O3	6.55	8.07	7.90	7.05	9.76	6.47	7.19	10.99	9.81	10.73	13.46	10.53	10.96	10.91	12.08	13.05	13.71
MnO	0.18	0.14	0.14	0.16	0.16	0.12	0.13	0.21	0.21	0.24	0.14	0.18	0.22	0.20	0.18	0.17	0.21
MgO	2.08	4.57	4.03	2.70	5.99	1.94	2.24	4.01	3.35	3.24	4.95	2.99	4.22	5.76	4.76	5.67	3.41
CaO	10.09	7.67	5.03	4.14	8.09	4.72	1.48	6.80	6.93	8.33	6.90	6.73	6.52	6.62	4.22	5.36	4.42
Na2O	3.40	2.71	3.39	5.95	4.06	4.28	3.67	3.51	1.63	4.63	3.78	4.29	2.70	3.94	3.77	4.51	4.84
K2O	0.89	1.03	4.92	1.78	0.97	1.83	3.15	2.08	2.94	0.57	0.93	1.73	2.44	0.79	1.95	0.28	0.60
P2O5	0.46	0.16	0.18	0.55	0.21	0.16	0.20	0.21	0.17	0.08	0.16	0.16	0.21	0.19	0.15	0.15	0.27
LOI	4.66	2.92	3.09	3.00	2.46	3.01	5.04	4.02	11.73	13.36	9.03	4.00	10.42	4.88	6.14	7.10	5.17
TOTAL	99.94	99.95	100.02	99.79	99.53	99.13	99.62	99.00	99.97	98.87	99.63	99.27	99.21	99.23	99.62	98.99	99.53
FeO	3.00	4.65	5.05	5.46	6.64	3.07	4.63	6.10	4.48	5.40	10.30	3.79	6.28	5.75	7.09	8.51	7.07
H2O+	4.20	2.52	2.24	2.42	2.51	2.25	3.38	3.73	2.07	0.33	4.66	2.84	3.14	3.63	3.84	4.46	2.67
H2O-	0.67	0.23	0.28	0.44	0.22	0.30	1.19	0.18	0.12	0.04	0.13	0.02	0.06	0.06	0.06	0.08	0.08
Au(ppb)	5	4	44	1	<1	2	6	8	6	2300	19	6	7	9	3	4	6
Ag(ppm)	<0.2	0.2	0.2	0.2	0.2	<0.2	<0.2	<0.2	<0.2	1.0	<0.2	<0.2	<0.2	<0.2	<0.2	<0.2	<0.2
As(ppm)	12	16	16	2	20	<2	8	<2	4	4	2	<2	2	6	<2	2	2
Cu(ppm)	227	139	140	335	77	25	37	210	163	404	302	137	171	144	213	199	519
Fe(%)	3.89	3.54	4.23	4.37	3.58	3.52	4.62	5.81	5.08	6.99	7.81	5.16	5.97	5.27	6.91	7.02	8.18
Hg(ppm)	<1	<1	<1	<1	<1	1	<1	2	<1	<1	1	1	1	4	1	<1	2
Mo(ppm)	<1	<1	<1	<1	<1	<1	<1	<1	<1	<1	<1	<1	<1	<1	<1	<1	1
Pb(ppm)	6	<2	<2	<2	<2	6	6	4	4	6	4	4	6	2	2	2	2
S(%)	0.01	0.05	0.15	0.06	0.10	0.01	0.03	0.01	0.05	1.13	0.07	<0.01	0.01	<0.01	<0.01	<0.01	0.03
Sb(ppm)	<2	2	<2	<2	4	<2	<2	<2	<2	2	<2	4	<2	<2	<2	<2	<2
Zn(ppm)	68	62	66	90	50	90	98	94	92	104	114	102	116	104	100	104	134
							C. I. P. W. NORM										
Q	6.41	4.91	0.00	0.00	0.00	12.49	15.03	0.00	6.93	0.64	0.00	3.90	0.00	0.00	0.00	0.00	4.49
C	0.00	0.00	0.00	1.73	0.00	0.72	7.05	0.00	0.00	0.00	0.00	0.00	0.00	0.00	2.88	0.00	0.00
or	5.26	6.09	29.08	10.52	5.73	10.81	18.62	12.29	17.37	3.37	5.50	10.22	14.42	4.67	11.52	1.66	3.55
ab	28.77	31.39	28.69	50.35	34.35	36.22	31.05	29.70	13.79	39.18	22.36	36.30	22.85	33.34	31.90	37.25	40.95
an	35.54	27.65	18.11	16.95	26.39	22.37	6.04	30.93	26.02	4.87	26.73	20.00	25.20	26.12	19.96	25.18	16.59
ne	0.00	0.00	0.00	0.00	0.00	0.00	0.00	0.00	0.00	0.00	5.22	0.00	0.00	0.00	0.00	0.50	0.00
di	6.87	5.41	2.98	0.00	6.68	0.00	0.00	0.74	4.39	17.41	2.58	9.02	2.98	3.26	0.00	0.21	1.80
hd	2.40	2.15	1.64	0.00	3.38	0.00	0.00	0.43	1.43	8.63	2.80	0.67	1.74	1.15	0.00	0.15	1.15
wo	0.00	0.00	0.00	0.00	0.00	0.00	0.00	0.00	0.00	1.62	0.00	0.00	0.00	0.00	0.00	0.00	0.00
vn	2.00	8.87	0.80	2.47	0.30	4.83	5.58	0.44	6.31	0.00	0.00	3.27	3.70	9.13	7.45	0.00	7.66
fs	0.80	4.04	0.51	3.06	0.17	2.04	5.59	0.29	2.36	0.00	0.00	0.28	2.48	3.70	5.12	0.00	5.52
fo	0.00	0.00	5.50	2.98	8.08	0.00	0.00	6.45	0.00	0.00	7.80	0.00	3.80	2.60	3.09	9.83	0.00
fa	0.00	0.00	3.83	4.07	5.16	0.00	0.00	4.69	0.00	0.00	10.72	0.00	2.80	1.16	2.34	8.60	0.00
mt	4.67	4.20	3.22	1.42	3.45	4.44	2.96	6.10	7.00	6.86	2.91	9.16	5.77	6.55	6.09	5.20	8.48
il	1.27	1.41	1.50	1.35	2.15	1.48	1.69	1.75	1.73	2.15	2.47	1.65	1.86	1.60	1.99	2.03	2.77
ap	1.07	0.37	0.42	1.27	0.49	0.37	0.46	0.49	0.39	0.19	0.37	0.37	0.49	0.44	0.35	0.35	0.63
TOTAL	95.05	96.49	96.37	96.18	96.33	95.78	94.06	94.30	87.74	84.91	89.45	94.86	88.09	93.71	92.69	90.94	93.57
salic-total	75.98	70.04	76.87	79.56	66.48	82.62	77.78	72.92	64.12	48.06	59.80	70.43	62.47	64.13	66.26	64.58	65.58
femic-total	19.07	26.45	20.50	16.63	29.86	13.16	16.28	21.38	23.62	36.85	29.65	24.42	25.62	29.58	26.43	26.36	27.99
D.I.	40.44	42.39	57.77	60.87	40.08	59.52	64.70	41.99	38.09	43.19	33.08	50.42	37.27	38.01	43.42	39.40	48.99
S.I.	16.94	27.53	20.67	16.03	30.15	13.91	14.36	20.46	19.97	17.81	22.65	16.11	21.86	28.26	22.22	25.41	16.03
FeO*/MgO	2.83	1.59	1.76	2.35	1.47	3.00	2.89	2.47	2.63	2.98	2.45	3.17	2.34	1.70	2.28	2.07	3.62
Na2O+K2O	4.31	4.77	8.36	7.80	5.10	6.19	6.89	5.70	4.60	5.30	4.79	6.10	5.23	4.81	5.80	4.90	5.52

[Legend] D.I.:differetiation index S.I.:solidification index * total Fe as FeO
C.I.P.W. NORM : W. Cross, J.P. Iddings, L.V. Pirsson and H.S. Washington (1902)

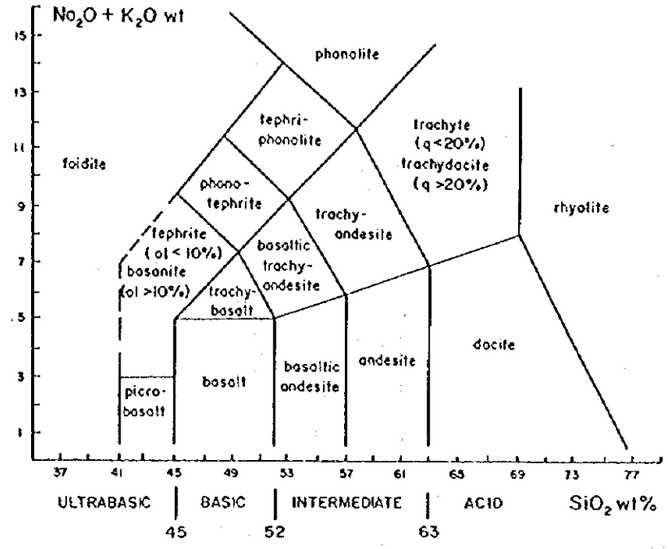

(Le Bas et al., 1986)

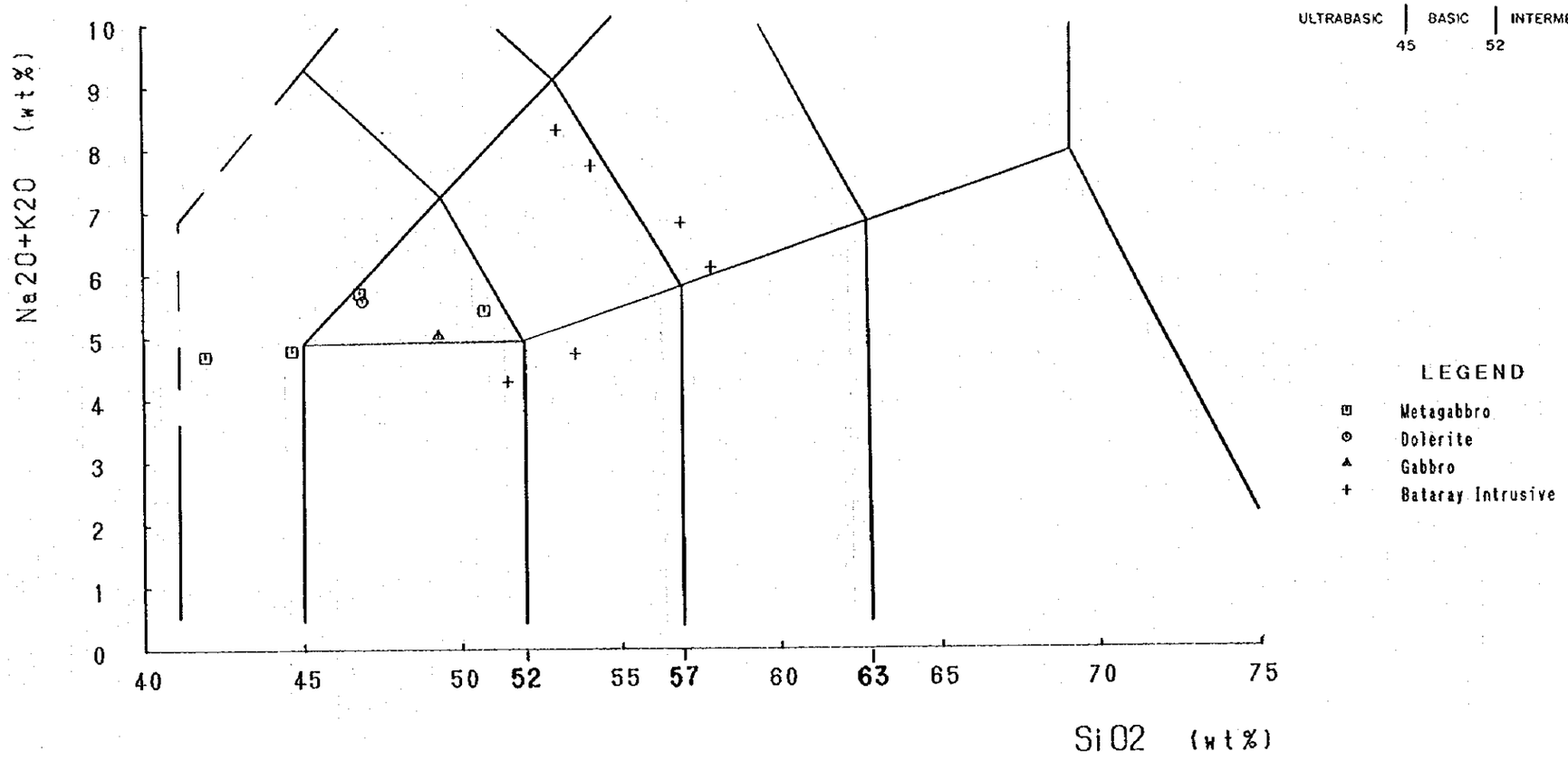

Fig. 13 TAS Diagram

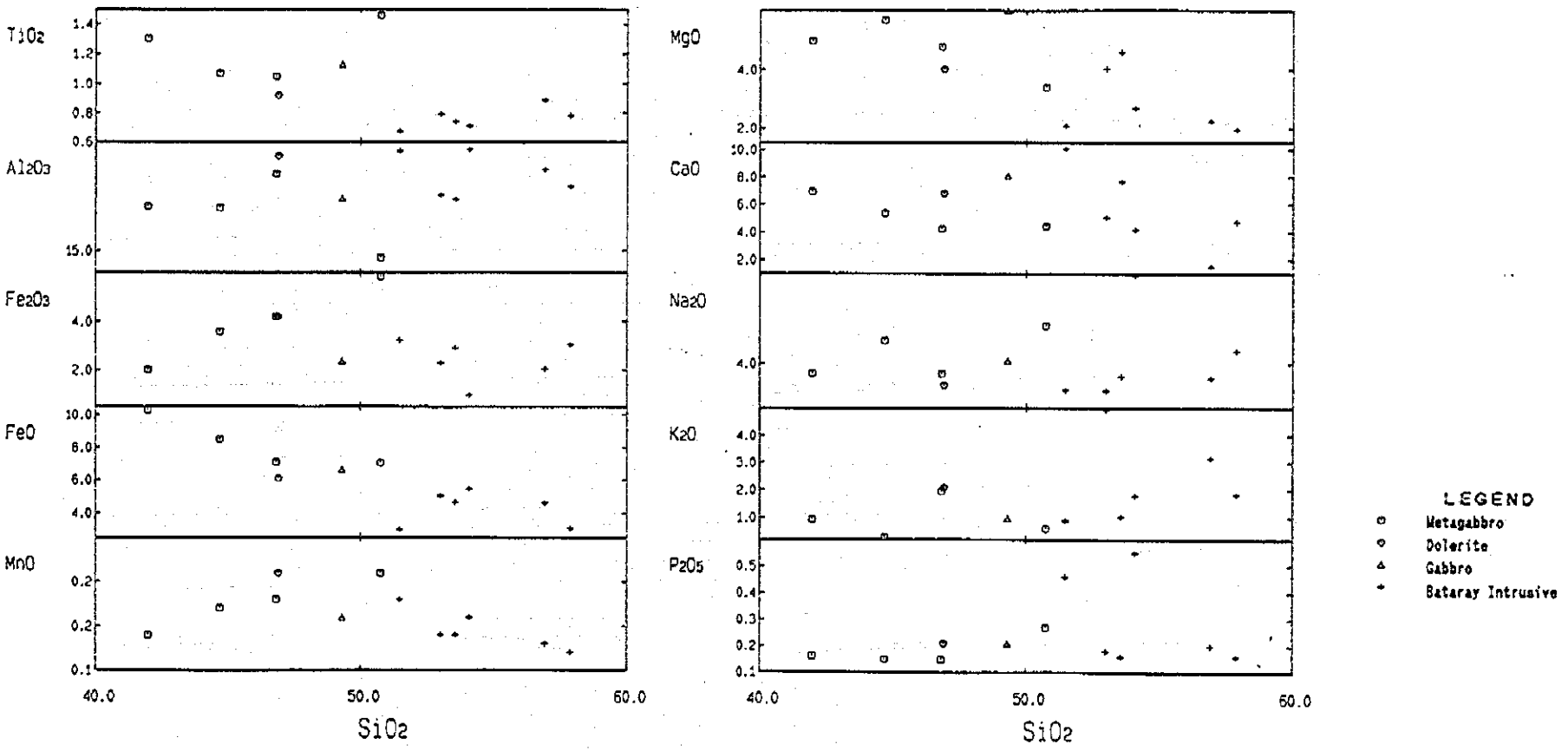

Fig. 14 Harker Diagram

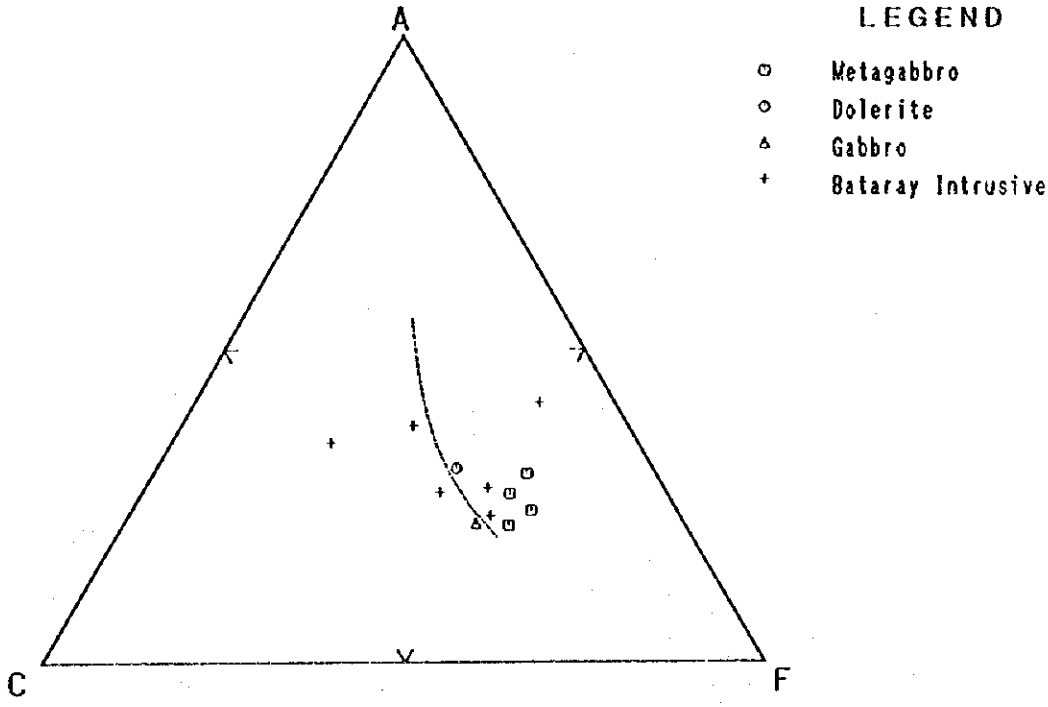

Fig. 15 ACF Diagram

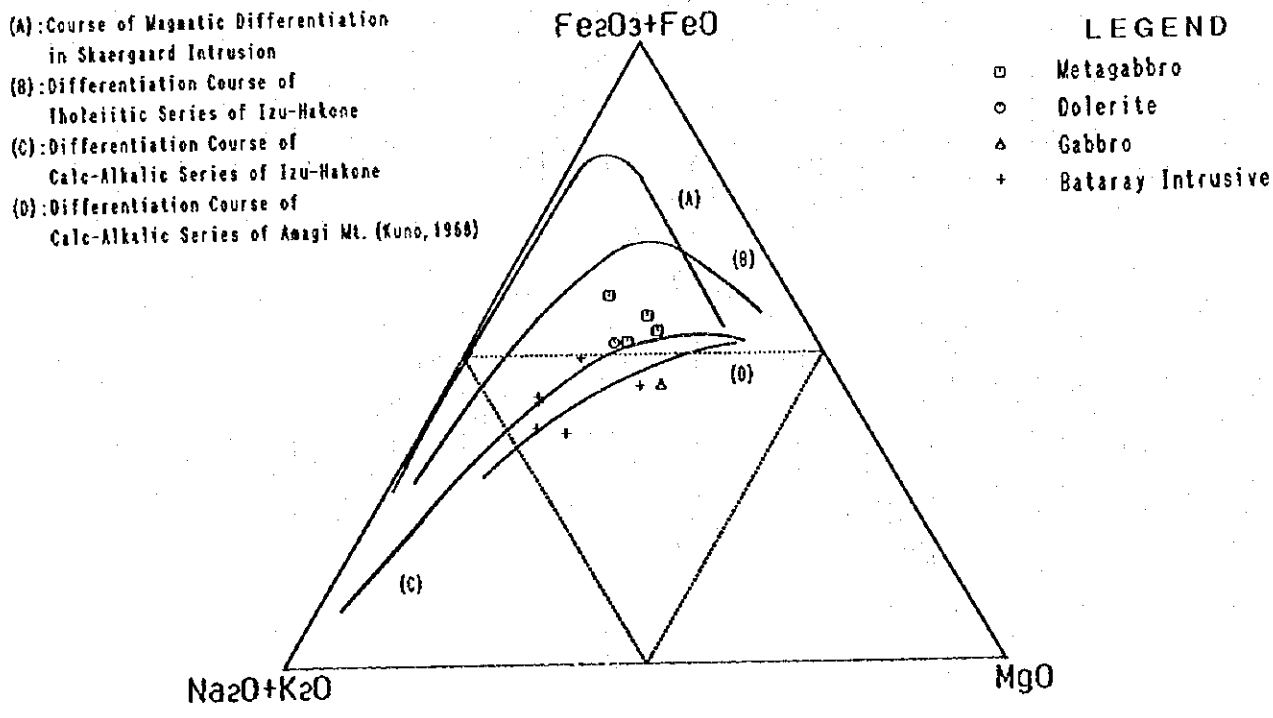

Fig. 16 MFA Diagram

Table 17 Results of Rare Earth Element Analysis

Sample No.		BC-2	KKR-9-1	KKR-9-2	3-18.75	5-27.85	5-33.15	5-44.95	5-60.00	5-74.20	7-48.75	9-67.50	12-44.50	OIB (*1)	コンドライト (*2)	コンドライト (*3)
Ba	ppm	250.0	215.0	745.0	80	65	60	245	150	160	170	45	115	150	6.9	—
Ce	ppm	23.0	28.0	20.0	18	21	19	21	28	24	16	15	26	35.5	0.865	0.957
Eu	ppm	1.0	1.0	1.0	1	1	1	1	1	1	1	1	2	1.88	—	0.087
La	ppm	10.0	15.0	11.0	8	10	8	10	12	10	7	6	11	13.4	0.328	0.367
Lu	ppm	0.2	0.3	0.3	0.2	0.3	0.3	0.2	0.3	0.2	0.3	0.2	0.5	—	—	—
Nb	ppm	2.0	8.0	8.0	2	2	2	2	2	2	2	2	2	17	0.35	—
Nd	ppm	15.0	16.0	12.0	14	15	14	13	20	16	11	11	18	10	0.63	0.711
Rb	ppm	60.0	24.0	40.0	44	12	16	34	40	16	32	6	12	9.2	0.35	—
Sm	ppm	4.1	4.3	3.7	3.4	4.2	3.8	3.6	4.4	4.1	3.2	3.1	5.4	—	—	—
Sr	ppm	1580.0	412.0	494.0	198	526	244	536	410	396	484	420	320	371	11.8	—
Tb	ppm	<0.5	0.8	<0.5	<0.5	0.6	<0.5	0.6	<0.5	<0.5	<0.5	<0.5	1	—	—	—
Th	ppm	1.0	2.0	2.5	1	<0.5	<0.5	1	1.5	1	0.5	0.5	1	—	—	—
U	ppm	<1.0	1.0	<1.0	<1.0	<1.0	<1.0	<1.0	<1.0	<1.0	<1.0	<1.0	<1.0	—	—	—
Y	ppm	16.0	24.0	20.0	16	24	20	16	18	16	18	16	26	25	2	2.25
Yb	ppm	2.0	2.5	2.5	2	3	2	2	2	2	2	2	3	1.98	0.22	0.248
Zr	ppm	87.0	120.0	132.0	69	87	81	78	84	72	78	75	123	115	6.84	—
Sr/Y		98.8	17.2	24.7	12.4	21.9	12.2	33.5	22.8	24.8	26.9	26.3	12.3	14.8	5.9	—

*1:Willson(1989), *2:Thompson R.N. et al.(1984), *3:Taylor and Mclennan(1985)

OIB: Ocean island basalt

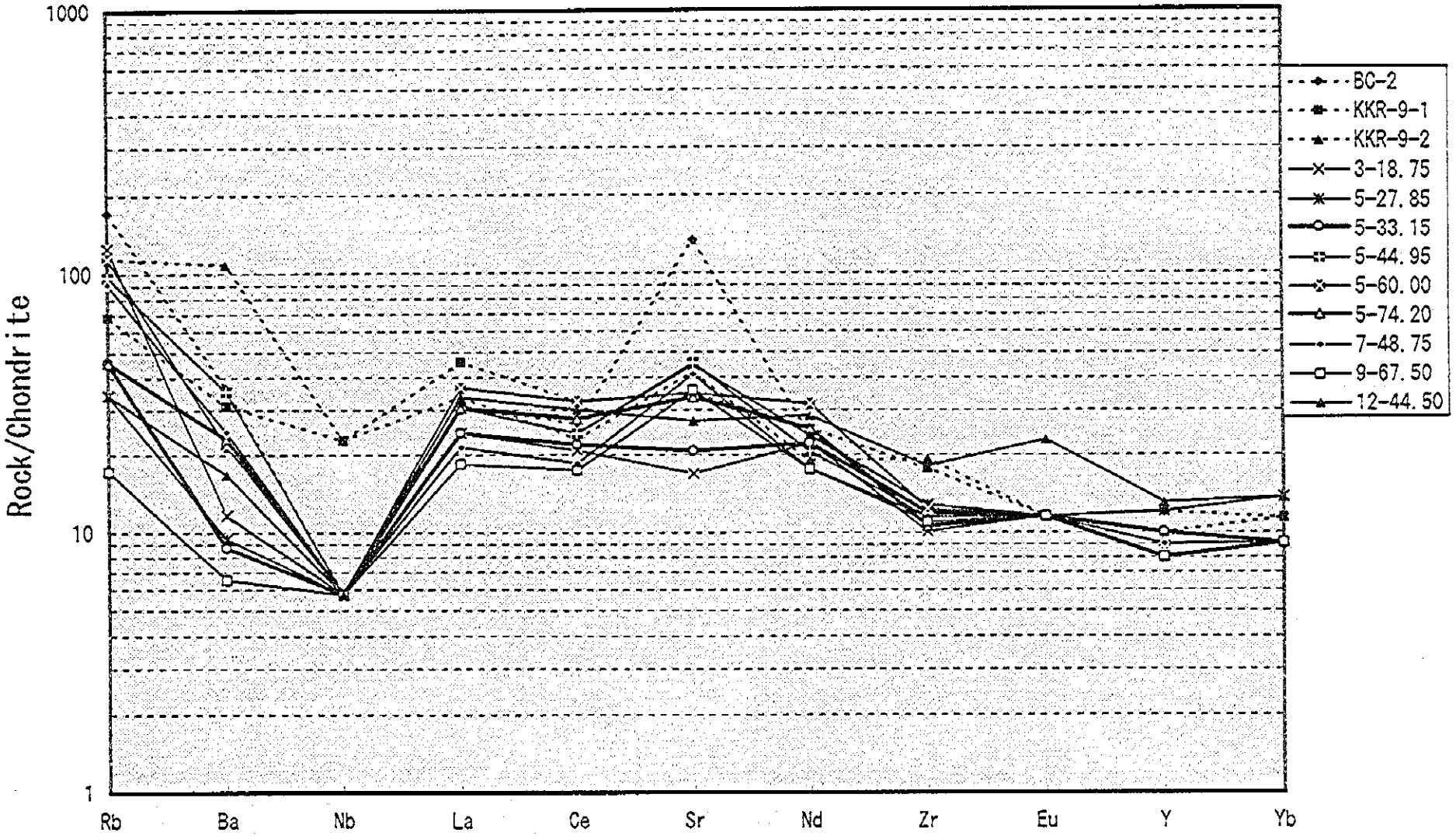

Fig. 17 Spidergram of Rare Earth Elements (REE pattern)

PART III CONCLUSIONS AND RECOMMENDATIONS

PART III CONCLUSIONS AND RECOMMENDATIONS

Chapter 1 Conclusions

1-1 Carorongan Area

(1) The geology of Carorongan Area is composed of greenschist and metagabbro of the Catanduanes Formation. The greenschist originated from shale, siltstone, sandstone and lapilli tuff which have basic composition. The schistosities generally show the NW-SE direction subparalleling the faults in sheared zone. The metagabbro has schistosities subparalleling the faults in sheared zone as those of the greenschist. The metagabbro usually occurs in the form of sheets in the Catanduanes Formation such as strata.

(2) The geological structure is characterized by NW-SE trending faults which are cut by E-W and NE-SW trending faults. The extended directions of sheared zone and silicified zone mainly define the NW-SE trend, but some quartz veins containing high gold grade have the E-W trend.

(3) From the results of trenching survey, the gold mineralization is said to be related to hydrothermal alteration and the quartz veins within the whole series of trenches. The direction of quartz veins is generally NW-SE and decreases in frequency to N-S, E-W and NE-SW, however the quartz veins with high Au grade are mainly in NW-SE and E-W directions. Within the trench T-3, the silicified zone containing 4.2 g/t Au and about 4 m in width is recognized and the quartz vein striking N75° E and dips 85° NW contains 58.8 g/t Au and about 15 cm in width.

(4) From the results of drilling survey, the silicified zones were found to continue to deeper levels from surface. The strongly silicified zones were proved to continue 30 m below the surface in 4 holes (MJPC-3, 4, 5, 6) which were carried out on platform 2. Some other silicified zones exist at deeper levels (44 - 86 m below the surface) than the above-mentioned silicified zone and were recognized in the holes MJPC-8 and 9 that were carried out on platform 3. Major portion of the mineralization usually occurs within the metagabbro intrusives and the contacts between the metagabbro and the greenschist.

(5) Based on the results of ore analysis, only Au has the high potential, though there are some samples containing slightly high concentrations of Cu and Zn. As to the Au grade, values of 1.5 g/t (MJPC-5, 26.80 - 30.85 m) were determined in the silicified zone at

shallower levels and values of 1.2 g/t (MJPC-8, 83.20 - 84.20 m) were determined in the silicified zone at deeper levels.

1-2 Kampayas Area

(1) The geology of Kampayas Area is mainly composed of sedimentary rocks of the Catanduanes Formation. These rocks are cut by the andesite porphyry and diorite of Batalay Intrusives. As to the mineralization, there are silicified zones and quartz veins in some places.

(2) The variation of each element on the geochemical survey in Kampayas Area is controlled by the NNE-SSW oriented fault, by the diorite body at the ridge around peak 379 m and by the strongly silicified zone at the eastern part of Kampayas creek. The NNE-SSW oriented fault passing by the ridge of peak 379 m could have served as channelways for the andesite porphyry and some hydrothermal solutions.

(3) As to the Au content, unaltered to weakly altered rocks yield values several times as compared with the Clarke number, and the strongly altered rocks are at dozens times. Of particular interest are the silicified rocks with high frequency of quartz veins wherein the quartz veins frequently yield values of 0.1 to 0.3 g/t Au. In Kampayas Area, the maximum Au value was determined in the quartz vein of about 20 cm in width along the NNE-SSW oriented fault passing by the ridge of peak 379 m. The value is 0.3 g/t Au.

(4) The results of K-Ar dating revealed the ages ranging from 33.6±2.1 Ma to 26.7± 0.6 Ma. These ages estimate for Batalay Intrusives correspond to middle to later period of Eocene. Based on these results, at least, the main mineralization in Kampayas Area occurred due to the hydrothermal activity related to Batalay Intrusives.

Chapter 2 Recommendations for Future Activity

2-1 Carorongan Area

It seems that the ore deposits recognized in Carorongan Area is sub-economical to develop at present because the deposits are slightly low gold grade as a whole and of limited size particularly concerning the high gold portions. It is notable, however, the gold contents of the metagabbro tend to be more than 0.1 g/t where the metagabbro was altered. Therefore, Carorongan Area and its vicinity must have a huge gold potential. At present, it is difficult to conclude whether the survey area was the centers of hydrothermal activity which brought about the gold mineralization or not.

After the detailed survey, we must delineate the potential areas for gold mineralization near Carorongan Area. In this case, it is imperative that the junctions of the NW-SE oriented faults consistent with the extension of the silicified zones and the E-W or NE-SW oriented faults of later tectonism could be of highest potential.

2-2 Kampayas Area

In Kampayas Area, the highest gold potential areas are believed to be near the ridge of peak 379 m and at the intersection of the NNE-SSW and E-W oriented faults in the southern part of the survey area. In particular, the site for forming a gold deposit is preferable at the above-mentioned intersection of the faults because the big quartz veins of about 20 cm (0.3 g/t Au) to 1 m in width and geochemical high gold anomalies are observed in the vicinity of the intersection. Therefore, we recommend to continue the additional surveys such as geophysical survey or drilling survey.

It is highly possible that a promising gold mineralization exists at the relatively higher part (above the 200 m in altitude) in the following reasons; There are many soil samples yielding high values of 0.1 to 2.6 g/t Au at the ridge around peak 379 m and in the southern part. High gold anomalies (more than 10 g/t Au) were recognized by the stream sediments geochemical survey of the Second Phase Survey at the eastern creek of the ridge. The quartz vein (KCR-08) of about 1 m in width at 200 m in altitude includes fluid inclusions showing the temperature ranging from 203 to 285° C (Ave. 248° C) and has low value of 0.02 g/t Au. On the other hand, the quartz vein (KCR-09) of about 20 cm in width at 270 m in altitude shows fluid inclusions homogenizing at ranging from 189 to 262° C (Ave. 217° C) and has

relatively high value of 0.3 g/t Au. Therefore, it is recommended that the additional surveys be conducted above the 200 m in altitude.

Moreover, it is proposed that the geological and geochemical detailed surveys be conducted in the eastern extension of Carorongan Area and Kampayas Area because the geochemical high gold anomalies extend to the area.

REFERENCES

Angeles, Corned M. and Theodore, Levy G.(1980): Detailed Geological/Geochemical Survey of Tilled and Guiamlong Area in Catanduanes. MGB.

Angeles, Corned M. and Theodore, Levy G.(1983): Statistical Analysis of the Geochemical Data in Kaglatawan, San Miguel, Catanduanes. MGB, Region V.

Berkman, D.A.(1976): Field Geologists' Manual. The Australian Institute of Mining and Metallurgy.

Capistrano, P.M.(1951a): Geological reconnaissance of Catanduanes. Progress Report, Philippine Bureau of Mines.

Capistrano, P. M.(1951b): Preliminary Report on the A.A.R. Botelho Coal Claim, Hitoma, Caramoran, Catanduanes. MGB.

Capistrano P. M.(1952): Notes on the Mineral Resources of Catanduanes Island. The Philippine Geologist, Vol. VI, No.4, the Geochemical Society of the Philippines, Manila.

Crispin, O.A., Weller, J.M. and Ibanez, C.B. (1955): Geology and coal resources of the Panganiban region, Catanduanes. Philippine Bureau of Mines Special Project Series Publication No. 2.

Govett, G.J.S.(1983): Handbook of exploration geochemistry, Volume 2. Statistics and Data Analysis in Geochemical Prospecting. ELSEVIER SCIENTIFIC PUBLISHING COMPANY, p.437.

JICA and MMAJ(1994): Report on the cooperative mineral exploration in the Catanduanes area, the Republic of the Philippines, Phase I. Japan International Cooperation Agency and Metal Mining Agency of Japan.

JICA and MMAJ(1995): Report on the cooperative mineral exploration in the Catanduanes area, the Republic of the Philippines, Phase II. Japan International Cooperation Agency and Metal Mining Agency of Japan.

Kajitani, Yuji (1993): Environment of Mining Investment in the Philippines(part 2). Mineral Information Center, Metal Mining Agency of Japan.

LeBas, M.J., LeMaitre, R.W., Streckeisen A. and Zanettin, B.(1986): A chemical classification of volcanic rocks based on the total alkali-silica diagram. J. Petrol., 27, 745-750.

Lepeltier, C.(1969): A simplified statistical treatment of geochemical data by graphical representation. Econ. Geol., 64, 538-550.

Levinson, A.A.(1974): Introduction to Exploration Geochemistry.

Meek, W.B.(1938): Report on the Geological Survey and Investigation of copper prospect in Agban, Catanduanes. Unpublished report, MGB.

Metal Mining Agency of Japan(1992): Geology and Mineral Resources of Southeast Asia-Oceanian Islands, 1991. Report of Geology Analysis Committee, Mineral Information Center, Metal Mining Agency of Japan.

MGB(1982a): Geology and Mineral Resources of Catanduanes Province. Report of Investigation No.108, Map and Mineral Resources Compilation Team, MGB, Region V.

MGB(1982b): Geology and Mineral Resources of the Philippines, Vol. 1.

MGB(1983a): Geological Map of Nagumbuaya Point Quadrangle, Sheet 3860 I. Bureau of Mines and Geo-Sciences, Ministry of Natural Resources.

MGB(1983b): Geological Map of Calolbon Quadrangle, Sheet 3860 IV. Bureau of Mines and Geo-Sciences, Ministry of Natural Resources.

MGB(1983c): Geological Map of Bagamanok Quadrangle, Sheet 3861 I. Bureau of Mines and Geo-Sciences, Ministry of Natural Resources.

MGB(1983d): Geological Map of Gigmoto Quadrangle, Sheet 3861 II. Bureau of Mines and Geo-Sciences, Ministry of Natural Resources.

MGB(1983e): Geological Map of Hitoma Quadrangle, Sheet 3861 III. Bureau of Mines and Geo-Sciences, Ministry of Natural Resources.

MGB(1983f): Geological Map of Caramoran Quadrangle, Sheet 3861 IV, Bureau of Mines and Geo-Sciences, Ministry of Natural Resources.

MGB(1983g): Geological Map of Pandan Quadrangle, Sheet 3862 III. Bureau of Mines and Geo-Sciences, Ministry of Natural Resources.

MGB(1985): Geological Map of Gibgos Quadrangle, Sheet 3761 I. Bureau of Mines and Geo-Sciences, Ministry of Natural Resources.

Mitchell, A.H.G. and Balce, G.R.(1990): Geological features of some epithermal gold systems, Philippines. Epithermal gold mineralization of the circum-pacific,1, p.241-296.

Nishido, H., Itaya, T. and Ogata, K.(1984): K-Ar age determination method. Bull. Hiruzen Res. Inst., No.9, 19-38.

Santos, V. de los, et al.(1955): Geology and Coal Resources of the Hitoma-Manambrag Region, Catanduanes. Bureau of Mines, Manila.

Santos,V. de los, et al.(1959): Memorandum report on the phosphate and manganese deposits, Catanduanes. Unpublished report, Bureau of Mines, Manila.

Sinclair, A.J.(1976): Application of probability graphs in mineral exploration. Special Volume No. 4, the Association of Exploration Geochemists.

Steiger, R. and Jaeger, E.(1977): Subcommision on geochronology, Convention on the use of decay constants in geo- and cosmo-chronology. Earth Planet. Sci. Lett., 36, 359-362.

Theodore, Levy G. et al.(1988): Preliminary Report on the Small-Scale Gold Mining Development Project in Catanduanes for the Period September 19 to December 18, 1988. MGB.

Teves, J.S. et al.(1949): Report on the investigation of rock phosphate and other mineral possibilities of Bohol. Philippine Geologist, Vol. III, No. 2.

Tompson, R.N., Morrison, M.A., Hendry, G.L. and Parry, S.J.(1984): An assessment of the relative roles of a crust and mantle in magma series; an elemental approach. Phil. Trans. Roy. Soc. London, A310, 549-590.

Torres, Mario A.(1978): Geologic Investigation of the Gold Property of Rajah Lahuy Mining Company at Gata, Caramoan, Camarines Sur. MGB.

United Nations(1992): The Philippines, a Prospectus for the International Mining Industry. United Nations Development Programme 1992, United Kingdom.

Wilson, M.(1989): Igneous petrogenesis- A global tectonic approach. Unwim Hyman, London, 466p.

Wolfe J.A.(1981): Philippine geochronology. Jour. Soc. Phil., Vol. 35, 1-30.